



NAM

Groningen Dynamic Model Update 2018

Quint de Zeeuw and Leendert Geurtsen

NAM

Datum June 2018

Editors Jan van Elk & Dirk Doornhof

General Introduction

The subsurface model of the Groningen field is used to model the first step in the causal chain from gas production to induced earthquake risk. It models the pressure response in the gas and water bearing reservoir formations to the gas extraction.

The reservoir model of the Groningen field was built in 2011 and 2012 and has a very detailed description of the faults in the field to support studies into induced earthquakes. The model was used to support Winningsplan 2013 (Ref. 1 to 3) and has since then been continuously improved (Ref. 4 and 6). This report describes the continuous improvement of the subsurface model of the Groningen field and in particular the effort to update and improve the history match.

Pressure decline in the field is an important driver for compaction and therefore subsidence. Compaction in turn affects stress and strain and is therefore of importance for the mechanism inducing earthquakes. The model therefore has an important role in the optimization of the gas withdrawal from the reservoir to reduce seismicity.

For Winningsplan 2013 and Winningsplan 2016, the model was reviewed by the independent consultant SGS Horizon. An extensive assurance review (Ref. 5) with opinion letter has been prepared by SGS Horizon.

References

1. Winningsplan Groningen 2013, Nederlandse Aardolie Maatschappij BV, 29th November 2013.
2. Technical Addendum to the Winningsplan Groningen 2013; Subsidence, Induced Earthquakes and Seismic Hazard Analysis in the Groningen Field, Nederlandse Aardolie Maatschappij BV (Jan van Elk and Dirk Doornhof, eds), November 2013.
3. Supplementary Information to the Technical Addendum of the Winningsplan 2013, Nederlandse Aardolie Maatschappij BV (Jan van Elk and Dirk Doornhof, eds), December 2013.
4. Groningen Field Review 2015 Subsurface Dynamic Modelling Report, Burkitov, Ulan, Van Oeveren, Henk, Valvatne, Per, May 2016.
5. Independent Review of Groningen Subsurface Modelling Update for Winningsplan 2016, SGS Horizon, July 2016.
6. Groningen Dynamic Model Update 2018, NAM, Henk van Oeveren, Per Valvatne and Leendert Geurtsen, September 2017



NAM

Title	Groningen Dynamic Model Update 2018		Date	June 2018
			Initiator	NAM
Autor(s)	Quint de Zeeuw and Leendert Geurtsen	Editors	Jan van Elk Dirk Doornhof	
Organisation	NAM	Organisation	NAM	
Place in the Study and Data Acquisition Plan	<u>Study Theme: Prediction Reservoir Pressure based on gas withdrawal</u> <u>Comment:</u> The subsurface model of the Groningen field is used to model the first step in the causal chain from gas production to induced earthquake risk. It models the pressure response in the gas and water bearing reservoir formations to the gas extraction. The reservoir model of the Groningen field was built in 2011 and 2012 and has a very detailed description of the faults in the field to support studies into induced earthquakes. The model was used to support Winningsplan 2013 (Ref. 1 to 3) and has since then been continuously improved (Ref. 4 and 6). This report describes the continuous improvement of the subsurface model of the Groningen field and in particular the effort to update and improve the history match. Pressure decline in the field is an important driver for compaction and therefore subsidence. Compaction in turn affects stress and strain and is therefore of importance for the mechanism inducing earthquakes. The model therefore has an important role in the optimization of the gas withdrawal from the reservoir to reduce seismicity. For Winningsplan 2013 and Winningsplan 2016, the model was reviewed by the independent consultant SGS Horizon. An extensive assurance review (Ref. 5) with opinion letter has been prepared by SGS Horizon.			
Directly linked research	<ul style="list-style-type: none">• Reservoir Compaction• Optimisation of the aerial distribution of production			
Used data	Sub-surface data from the Groningen field; open-hole logs, core data, pressure data, production data etc.			
Associated organisation	Independent consultant SGS Horizon			
Assurance	For Winningsplan 2013 and Winningsplan 2016, the model was reviewed by an independent consultant SGS Horizon.			



NAM

Nederlandse Aardolie Maatschappij B.V.

Shell UPO

Groningen Dynamic Model Update 2018 – V5

Date: June 2018

Issued by: Quint de Zeeuw, Leendert Geurtsen

Executive summary

This note describes the Groningen field V5 dynamic subsurface model, with a focus on the changes with respect to the V4 model. The V5 model is used for the November 2017 Hazard and Risk Assessment, the January 2018 scenario modelling, and the 2018 update of Winningsplan 2016.

Two new elements have been incorporated in the V5 model:

- An updated static model, with reservoir properties based on a new seismic inversion iteration
- Rock properties including the Zeerijp-3A special core analysis results.

The new static model was up-scaled and history-matched until 30 April 2017 with respect to the following historical dynamic data:

- Static down-hole pressure measurements (SP(T)G),
- Repeat formation test pressures (RFT),
- Closed-in tubing-head pressures converted to bottom-hole pressures (CITHP-to-CIBHP),
- Interpreted rise in gas-water contact (PNL),
- Stable subsidence data from 2 levelling surveys (time-lapse from 1972 to 2013)
- Time-lapse gravity data (1996 and 2015)

The GIIP of the best-match dynamic model is 2938.4 N.Bcm. For the pressure match, focus shifted more towards the (high resolution) CITHP-to-CIBHP data, in order to better capture production induced transient effects around production clusters. The overall match to field pressures is:

- SPG RMS = 2.11 bar
- CITHP-to-CIBHP RMS = 1.35 bar

The V5 model does not include gas in the aquifer in the North of the field, nor the gas-bearing Carboniferous in the South of the field. Both features may have a significant impact on the model's dynamic behaviour. It is believed that the inclusion of these dynamic effects would be able to improve the match as currently obtained on the following parameters:

- RFT RMS = 11.88 bar
- PNL RMS = 2.44 meter
- Subsidence RMS = 1.87 centimetre
- Gravity RMS = 5.44 μ Gal

The following recommendations are made to further improve the model:

- Investigate the dynamic impact of depleting the gas bearing Carboniferous underneath the main Rotliegend reservoir,
- Incorporate gas in the aquifer of the dynamic model,
- Investigate an extension of the History Matching workflow with uncertainty indications for reservoir properties as derived from seismic information (semblance and inversion results).

These recommendations are expected to be implemented in a subsequent V6 update of the dynamic model, scheduled for August 2018. Time and progress permitting, two additional refinement steps are recommended:

- Include the gas in the aquifer and the gas-bearing Carboniferous interval in the dynamic reservoir model. Then include gravity data as a field-wide matching function in the history matching methodology.

- When an intermediate history match is obtained that reflects the effects from gas in the aquifer on water rise, run a new iteration of the seismic inversion with this dynamic model as a priori input to obtain an optimised porosity distribution.

Contents

Executive summary	3
1 Introduction.....	7
1.1 Background.....	7
1.2 Model objective.....	7
1.3 Readers guide	7
2 Updated model inputs.....	8
2.1 Property modelling from seismic inversion	8
2.2 Relative permeability model.....	8
2.2.1 Introduction	8
2.2.2 Available data.....	8
2.2.3 Relative permeability model	9
3 History matching – Methodology	11
4 History matching – Model updates and match.....	12
4.1 Relative permeability	12
4.2 Permeability multipliers	15
4.2.1 Regional permeability multipliers	15
4.2.2 North-East permeability multiplier	16
4.3 Fault seal factors	18
4.3.1 Overview	18
4.3.2 Northwest connectivity.....	20
4.3.3 Southwest connectivity	21
4.3.4 Kooipolder cluster fault	23
4.3.5 Rodewold depletion path.....	25
4.4 In place volumes.....	26
4.5 Reservoir pressure match	27
4.6 Water encroachment match.....	27
4.7 Subsidence match	27
4.8 Gravity match.....	29
5 Recommendations for future work.....	30
5.1 Update porosity from inversion of seismic data based on dynamic model including gas in the aquifer effects.....	30
5.2 Incorporation of Semblance and delta-thickness maps in History Matching workflow.....	30
5.2.1 Delta-thickness maps.....	30
5.2.2 Semblance map.....	31

5.3	Pre-existing recommendations	32
5.3.1	Gas in the aquifer.....	32
5.3.2	Carboniferous	32
5.3.3	Gravity data.....	33
6	References.....	34
	Appendix 1 – V5 best match	35
	Appendix 2 – Variable model parameter range and optimal V5 setting.....	36
	Appendix 3 – Model audit trail.....	39
	Appendix 4 – Permeability comparison of reservoir model versus build-up tests.....	40
	Appendix 5 – Harkstede block uncertainty	42

1 Introduction

1.1 Background

Following the 2012 Huizinge earthquake, NAM has initiated numerous technical studies to better understand the induced seismicity in the Groningen field, its causes, consequences, and possible ways of mitigation. Within this scope, the Groningen subsurface team finished the Groningen dynamic subsurface model V2.5 in 2016, Reference [1], linking subsidence to dynamic subsurface behaviour. This model was used as input to various studies, including the November 2015 Hazard and Risk Assessment and subsequent Winningsplan 2016 update. Furthermore, the model was used to generate forecasts for the 2016 Operating Plan and the 2016 Annual Review of Petroleum Resources.

As part of the Winningsplan 2016 submission, an update of the Study and Data Acquisition Plan was issued, Reference [2]. It outlined future studies into subsurface issues, offtake optimisation, and possible further improvements to the suite of models, including the dynamic reservoir model. NAM has committed to complete these studies. Most of the suggested improvements to the subsurface model have been incorporated into the V4 model update in 2017 [3], including;

- porosity based on inversion of seismic data,
- closed-in tubing head pressure data to match reservoir performance,
- a rock compressibility grid from model-based inversion of subsidence data and calculated reservoir pressure

The V4 dynamic model was used as the input to the 2017 production optimisation study which aimed to minimise production-induced seismicity (and associated risk) by controlling the field offtake at the cluster level within the constraints set by the Ministry of Economic Affairs. Additionally, the model was used for production forecasting, in support of the 2017 Operating Plan and 2017 Annual Review of Petroleum Resources.

The V5 dynamic model as described in this document provides an update to the V4 model by inclusion of the latest results of the Zeerijp-3A special core analysis program [4] and a new porosity grid from a second-pass inversion of seismic data. With the increasing importance of transient pressure effects at a cluster level (e.g. in regard of the risk based production optimisation work), the choice has been made in the V5 dynamic model to put more emphasis on the (late life CITHP) pressure match in the production clusters and less emphasis on the SPG match in observation wells, as described in section 4.2.2.

There are three elements remaining in the Study and Data Acquisition plan that are planned to be studied as part of the subsequent V6 dynamic model update as described in sections 5.3.1 to 5.3.3. In addition, two further recommendations for subsequent model updates are given in this document (sections 5.1 and 5.2).

1.2 Model objective

The V5 dynamic model update is used for evaluating the reservoir pressure response to production scenarios as part of the November 2017 Hazard and Risk Assessment, the January 2018 scenario modelling, and the 2018 update of Winningsplan 2016.

1.3 Readers guide

This report aims to highlight the differences between the V5 and the V4 model, and is best read in conjunction with Reference [3].

2 Updated model inputs

2.1 Property modelling from seismic inversion

In order to avoid a potential bias, external reviewers (SGS Horizon, TNO) have encouraged NAM to not base the distribution of reservoir properties on measurements from wireline logs only, since wells are typically targeting for the better quality rock and local highs. In the V4 dynamic model, the porosity grid in areas with limited well control was based on the results of a seismic inversion for porosity.

The seismic inversion process matches a synthetic seismic cube derived from the static model to measured seismic data. The seismic inversion optimization algorithm can vary static model properties such as porosity and/or reservoir thickness to improve the match. The output comprises a porosity cube and a set of reservoir zone boundary surfaces that resulted in an optimum fit.

In the V5 model, porosity was further updated based on a second iteration of the seismic inversion, as recommended in the V4 model update. In this second iteration, the porosity grid from the V4 model was used as a priori input in the inversion process. The second pass update aims to:

- Increase the overall energy available in the field by increasing porosity.
- Improve the connectivity between the Bierum production cluster and the observation wells De Hond and Uithuizermeeden, by increasing permeability in the North-East. Permeability is generated based on the new porosity grid and the existing porosity-permeability relationship derived from core measurements.

From these inversion results, only the porosity cube was used to steer the porosity distribution in the V4 and V5 static models. The adjustments in reservoir thickness were not reflected.

2.2 Relative permeability model

2.2.1 Introduction

The Zeerijp-3A well was drilled in 2015 with a large part of the Rotliegend interval cored. Special Core Analysis was carried out on a selection of core plugs, aiming to further constrain the imbibition relative permeability curves for the Groningen field. In addition, the ZRP-3A SCAL program included a Steady State primary drainage experiment, to allow for the option to implement/constrain hysteresis if so required. All parameters used to capture the full imbibition relative permeability curves in the Corey functions as assigned in GFR2015 [1] were reviewed and, if necessary, updated in line with the ZRP-3A SCAL experimental results to.

2.2.2 Available data

Prior to the Zeerijp-3 SCAL program, an overview of the relative permeability end points and Corey exponents from centrifuge and displacement (unsteady state) experiments as performed on multiple Groningen and Norg cores, together with the steady state experiment results, was given in overview reports [5] and [6]. At this point in time, only one single steady state experiment was available from a core sample of well ZPD-12, Reference [7]. The data was complemented by using Shell's in-house relative permeability database RELATE to obtain additional values for relative permeability end-points and Corey exponents from analogue fields in the Northern Netherlands.

The 2015-2016 Zeerijp-3A SCAL program provided several additional experiments to constrain the relative permeability model:

- 1 Steady-State Brine-Gas Imbibition experiment.
- 3 Steady-State Brine-Decane Imbibition experiments.

- 1 Steady-State Decane-Brine Primary Drainage experiment.
- 5 Toluene-Air Counter Current Imbibition experiments on 5 different plugs, using initial gas saturations of 20%, 40%, 60%, 80% and 100%.

The relative permeability model for the V5 model was updated based on Groningen cores only, both steady state and unsteady state experiments, including the results from the Zeerijp-3 SCAL program [4].

2.2.3 Relative permeability model

Relative permeability is modelled with the Corey functions:

$$k_{rw} = k_{rw,e} \left(\frac{S_w - S_{wc}}{1 - S_{wc} - S_{gr}} \right)^{N_w}$$

$$k_{rg} = k_{rg,e} \left(\frac{1 - S_w - S_{gr}}{1 - S_{wc} - S_{gr}} \right)^{N_g}$$

where

k_{rw}	water relative permeability
k_{rg}	gas relative permeability
$k_{rw,e}$	water endpoint relative permeability
$k_{rg,e}$	gas endpoint relative permeability
S_w	water saturation
S_{wc}	connate water saturation
S_{gr}	residual gas saturation
N_w	water Corey exponent
N_g	gas Corey exponent

The L/B/H ranges for all Corey parameters are listed below in Table 1. Figure 2-1 shows the associated Corey curves for V5. Figure 2-2 shows the fractional flow curves for V5 as well as the fractional flow curves for V4 for reference. Please note that in the assisted history matching workflow used for V5, each parameter (e.g. S_{gr} , k_{rwe} , etc.) is independently varied within its L/B/H range.

Table 1 L/B/H range for Corey parameters used in V5 history matching workflow

	Base	Low	High
Swc	$S_{wc} = 1.7408 * \phi^2 - 1.2617 * \phi + 0.2884$		
Sgr	$S_{g,r} = 0.35 * (0.357 - \phi) + 0.22$	$S_{g,r} = 0.7 * (0.357 - \phi) + 0.22$	$S_{g,r} = 0.22$
krwe	0.377	0.534	0.071
krge	0.656	0.565	0.860
Nw	4.0	3.5	4.5
Ng	2.3	3.0	1.5

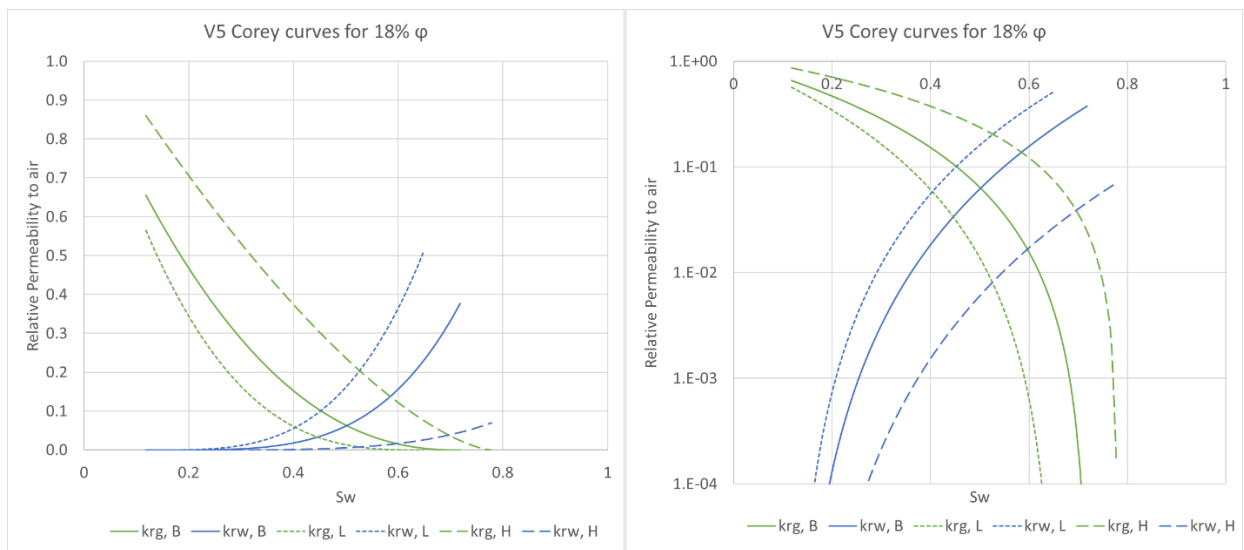


Figure 2-1 Different sets of Corey curves resulting from L/B/H parameters as from Table 1

Fractional flow curves V4 vs. V5

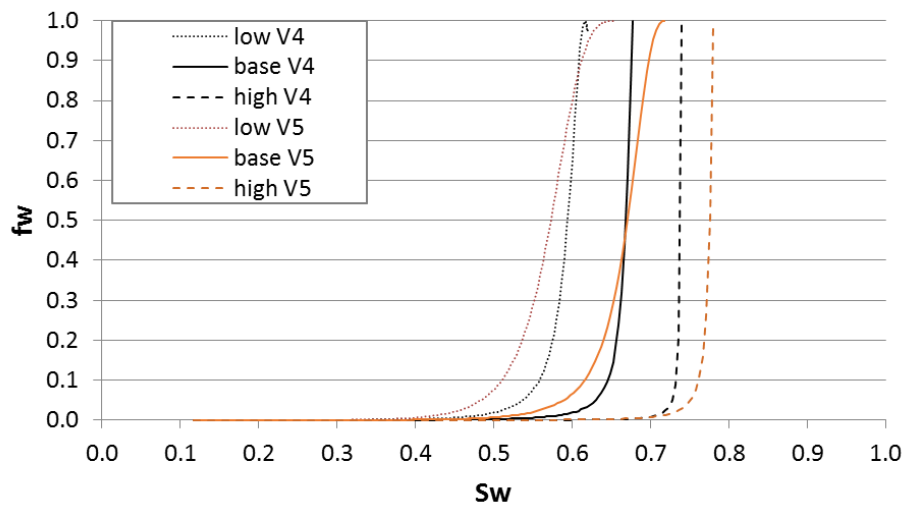


Figure 2-2 Fractional flow curves resulting from combining L/B/H case parameters for V4 and V5.

3 History matching – Methodology

For the V5 model update, a similar history matching method was applied as for the V4 model update. This method was described in detail in the GFR2015 report [1]; the extension of the history matching method with the Adjoint method was described in the report on the V4 model update [3].

4 History matching – Model updates and match

The main model updates resulting from the history matching process with reference to the V4 model are highlighted in paragraphs 4.1 to 4.4 below. The high level matching indicators are given in paragraphs 4.5 to 4.8, and detailed visualizations of the actual best match are summarized in Appendix 1.

4.1 Relative permeability

History matching the V5 model resulted in the relative permeabilities as summarized in Table 2. Figure 4-1 shows the best match relative permeability curves for 18% porosity.

Table 2 V5 and V4 best matched relative permeability model parameters

	V5 Best match	V4 Best match
Swc	$1.7408 * \phi^2 - 1.2617 * \phi + 0.2884$	$1.7408 * \phi^2 - 1.2617 * \phi + 0.2884$
Sgr	0.22	0.26
krwe	0.377	0.400
krge	0.860	0.890
Nw	4.0	3.0
Ng	1.5	1.4

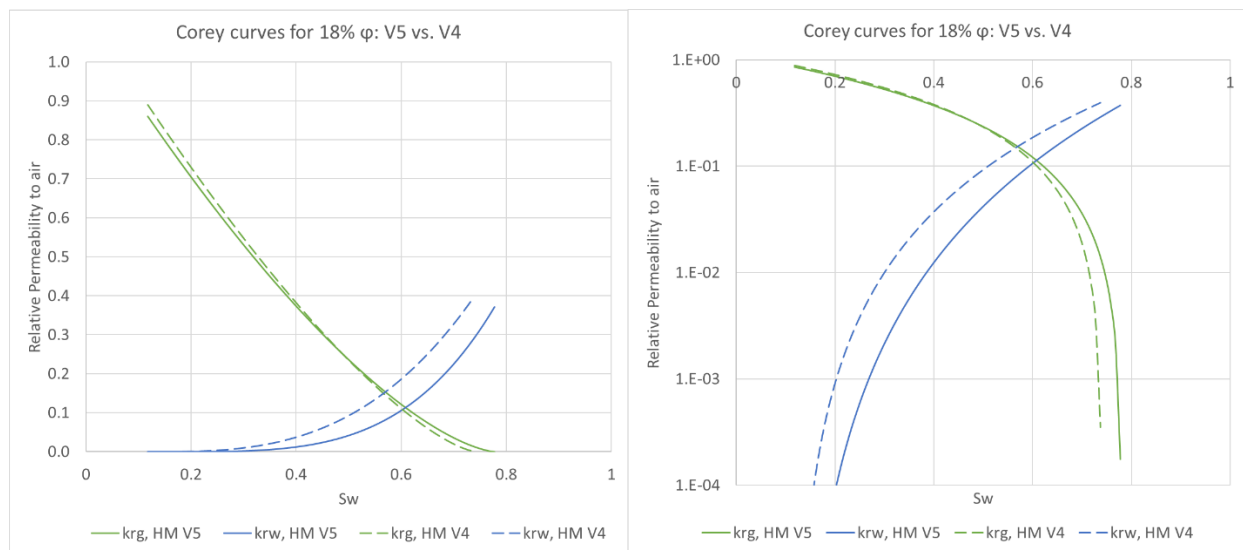


Figure 4-1: V5 and V4 best matched relative permeabilities for 18% porosity

Fractional flow curves

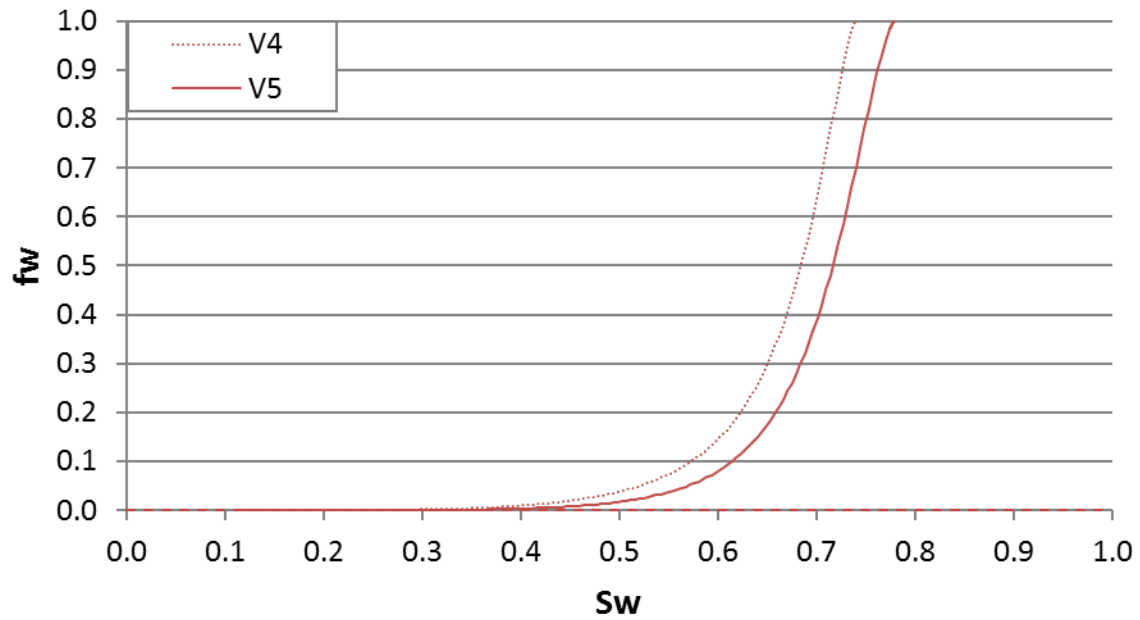


Figure 4-2 Fractional flow curves for V5 and V4 best matched relative permeabilities for 18% porosity

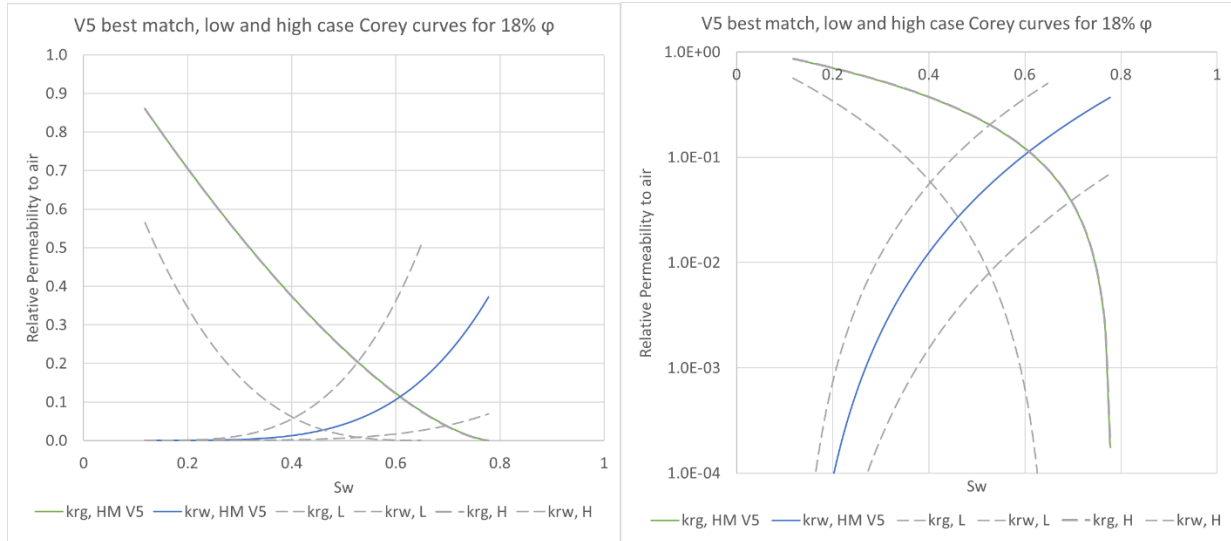


Figure 4-3: V5 best matched relative permeabilities for 18% porosity plotted within low case/high case envelope.

Fractional flow curves

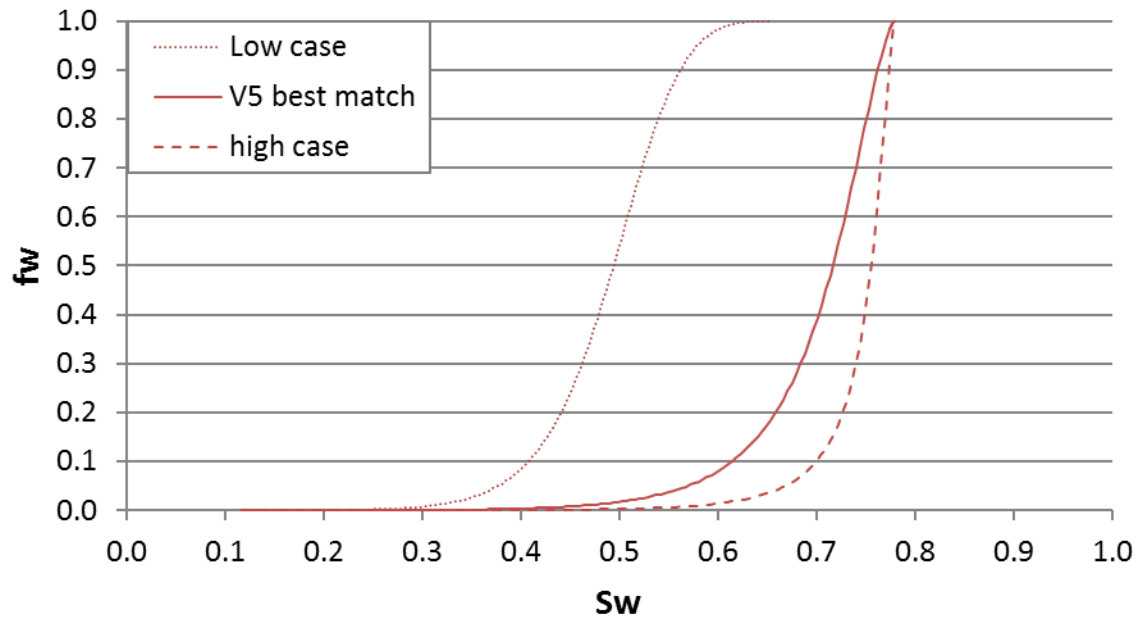


Figure 4-4: Fractional flow curves for V5 best matched relative permeabilities for 18% porosity plotted within low case/high case envelope.

4.2 Permeability multipliers

4.2.1 Regional permeability multipliers

History matching the dynamic model required a relatively consistent upward adjustment of the static model permeabilities by a factor of 2-3 throughout the field (Figure 4-5). This is within the uncertainty ranges from the scale difference in core data and the reservoir as a whole. However, in the “Central area” a larger increase in permeability was required (factor of ~5). This requirement for relatively large permeability values in the Central area has been consistent throughout the recent modelling updates and is explained further in the V4 model update report [3].

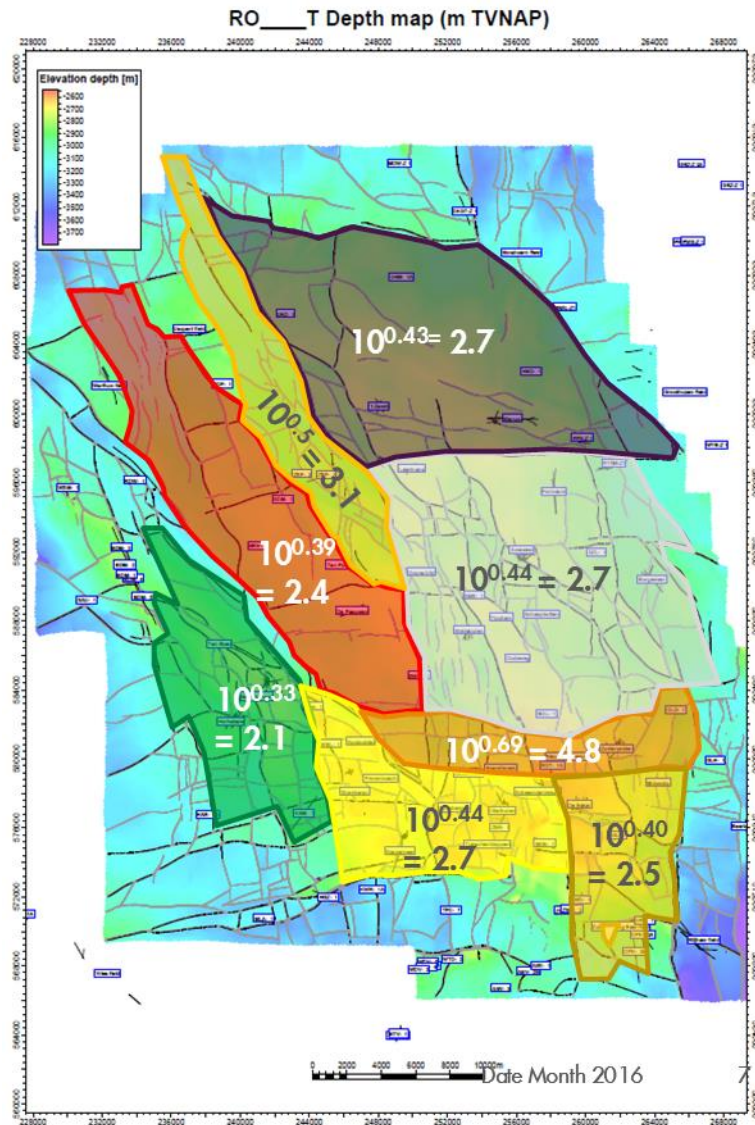


Figure 4-5 Permeability multipliers as applied in the V5 model

4.2.2 North-East permeability multiplier

The second pass seismic inversion was meant to test whether a better connectivity in the north of the field could be established. This was to provide a match in the northern production wells as well as the northern observation wells, as recommended in the V4 report. However, with the updated property model in the V5 model, a match on northern production clusters is still mutually exclusive to a match on the northern observation wells (an overview of the area is given in Figure 4-6).

The V4 model puts more emphasis on the pressure match in the observation wells de Hond and Uithuizermeeden, but the choice was made in V5 to preferentially honour the late life pressure behaviour from CITHP at 't Zandt and Bierum production clusters, see Figure 4-7. This alternative behaviour was achieved by applying a permeability multiplication factor of 2.7 in the north of the field, as compared to the relatively high factor of 4.2 for the V4 model. The lower multiplication factor is more in line with multipliers in the rest of the field for the V5 model and the lower permeabilities observed in the well tests, see Appendix 4.

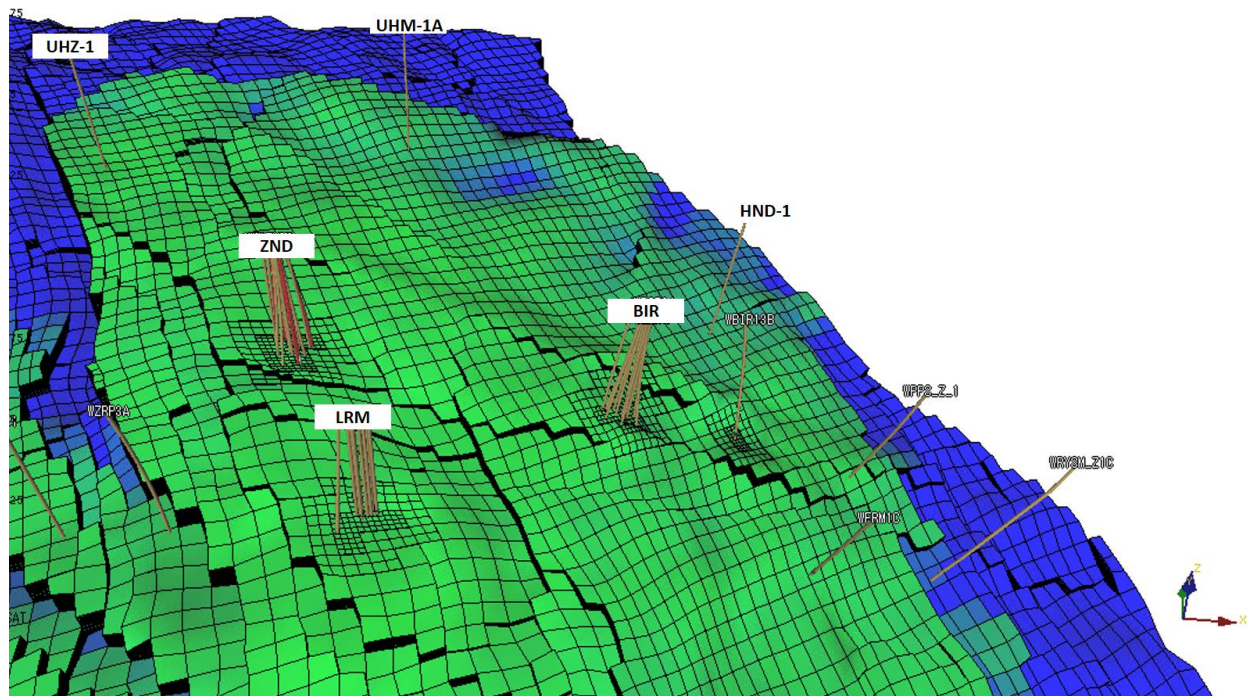


Figure 4-6: Saturation grid in the North-East of the reservoir

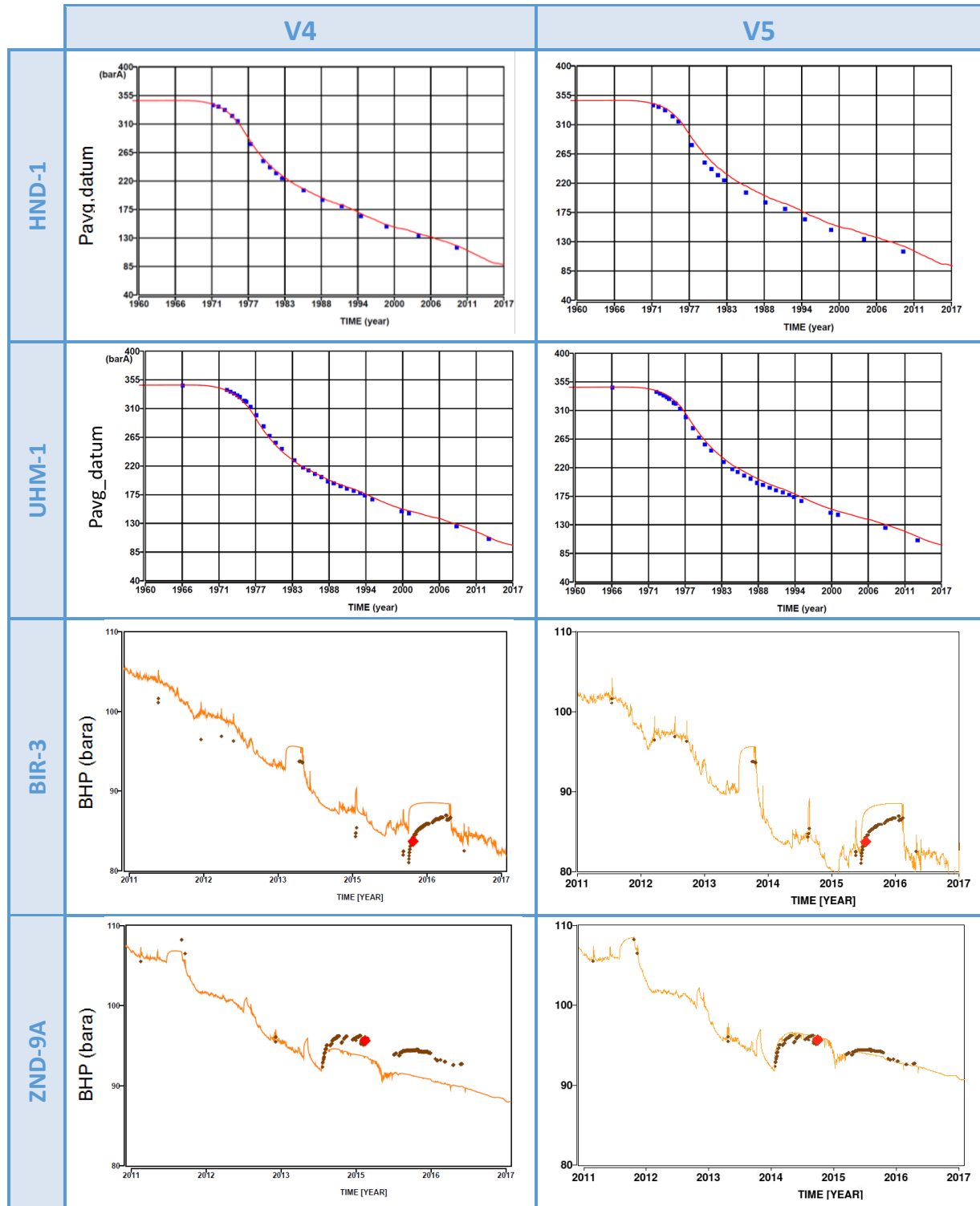


Figure 4-7: Pressure match in the Northeast for the V4 (left) versus the V5 (right) model. Top: SPG matches in HND-1 and UHM-1; bottom: CITHP matches in BIR-3 and ZND-9A.

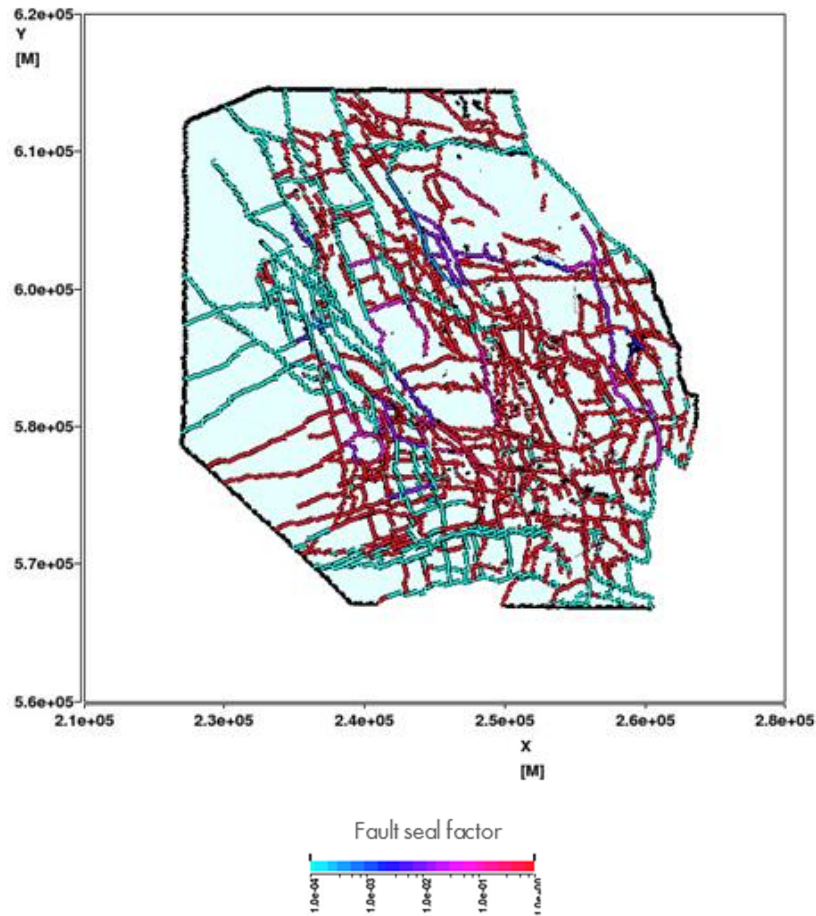
4.3 Fault seal factors

4.3.1 Overview

The V5 model builds on the fault seal factor multipliers from the V4 model, but introduced some further modifications. Figure 4-8 gives an overview of the fault seal factors obtained from the V5 history matching process.

Color scale clipped to highlight:

(A) more sealing faults



(B) less sealing faults

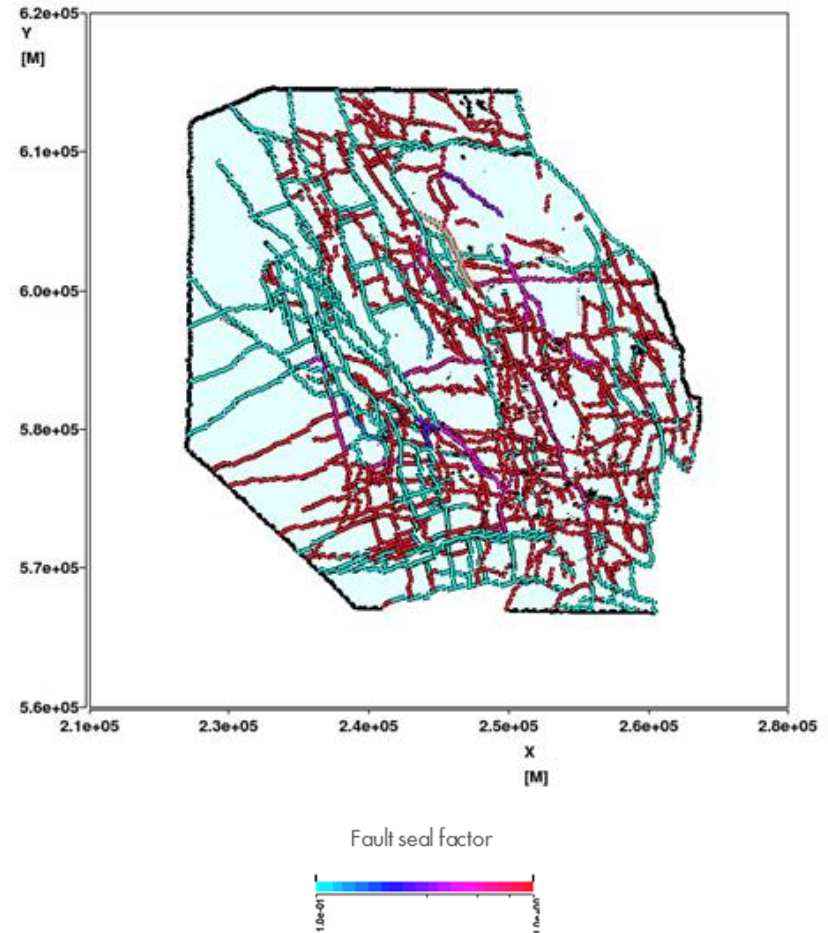


Figure 4-8 Fault seal factors in the Groningen V5 dynamic model. Warm colours indicate more open faults, cold colours indicate more sealing faults

4.3.2 Northwest connectivity

The Adjoint method was applied within the V4 modelling workflow and described in the V4 report [3]. A similar Adjoint calculation was run on the V5 model. It indicated that a reduction in connectivity is needed between the Ten Post, De Pauwen and Overschild production clusters, see Figure 4-9. In Figure 4-10 it is shown that this reduction is aligned with a large fault (125 meter throw) in between these production clusters. A fault seal factor multiplier was assigned to this fault in the history matching process.

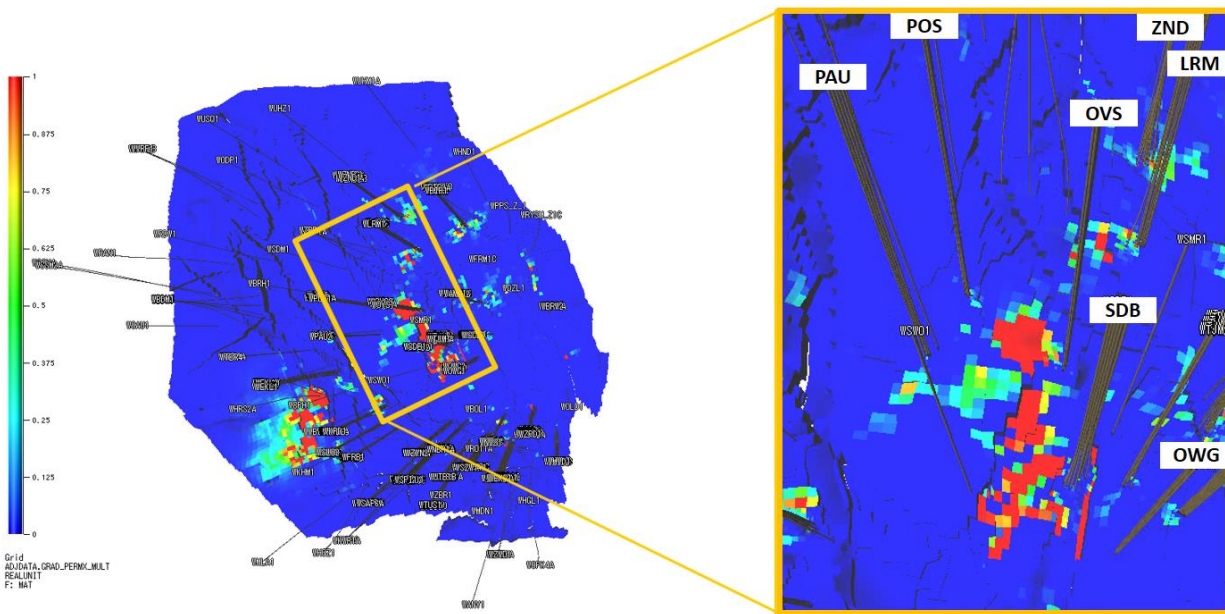


Figure 4-9 Positive permeability gradient with respect to pressure. A positive gradient will indicate reductions necessary to reduce the mismatch.

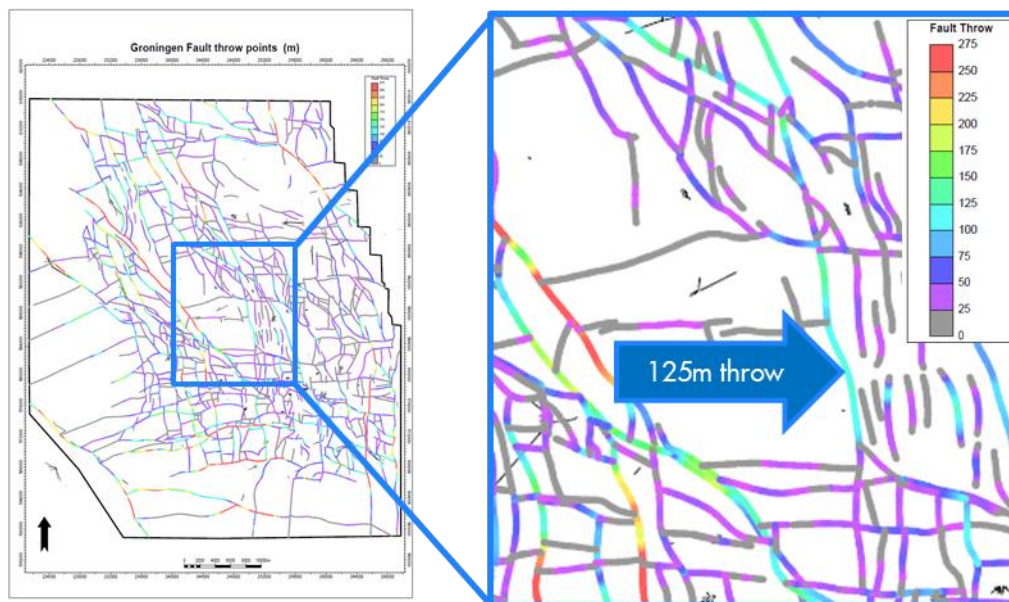


Figure 4-10 Groningen field fault throw map and zoom-in between Ten Post/ De Pauwen and Overschildt production clusters.

4.3.3 Southwest connectivity

From CITHP data it was observed that there is a 3-5 bar pressure lag within the Southwestern area of the field between West (clusters Kooipolder, Slochteren, Froombosch and Sappemeer) and East (clusters Spitsbergen and Tusschenklappen), see Figure 4-11. These two areas are separated by a series of relatively large faults (>100m throw) which to the North are associated with the pop-up blocks, Figure 4-12 and Figure 4-13. In order to reproduce this pressure lag in the reservoir model, additional fault seal factors had to be applied.



Figure 4-11 Schematic indicating roughly CIBHPs at main clusters in the Groningen southwest area in December 2015, see CITHP2BHP match in Appendix 1 for more detailed pressures.

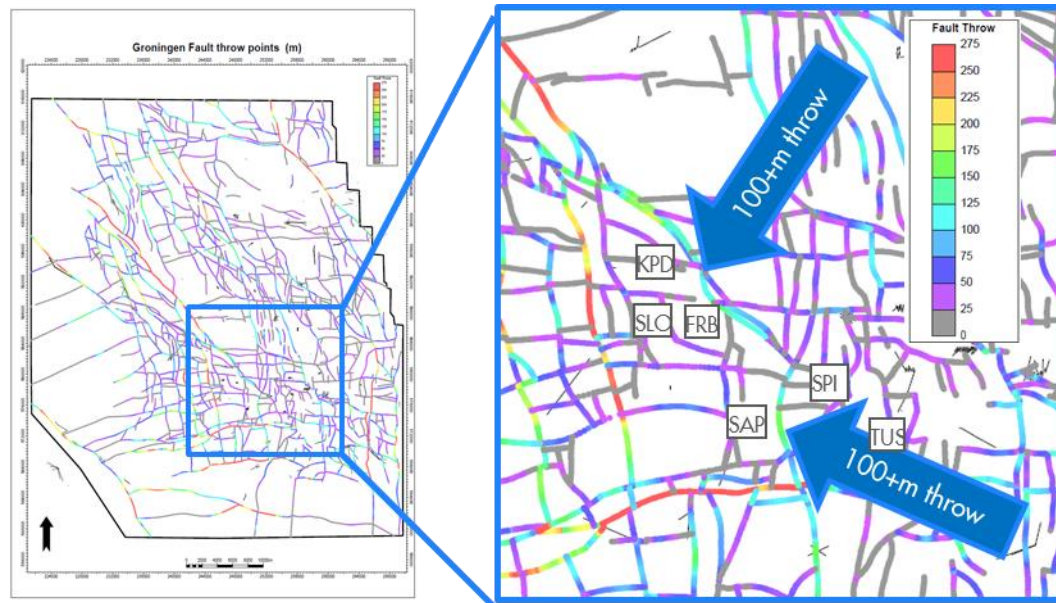


Figure 4-12 Groningen field fault throw map and zoom-in to Groningen southwest area. The 2 main faults separating the KPD,SLO,FRB and SAP clusters from the rest of the field are indicated by the blue arrows.

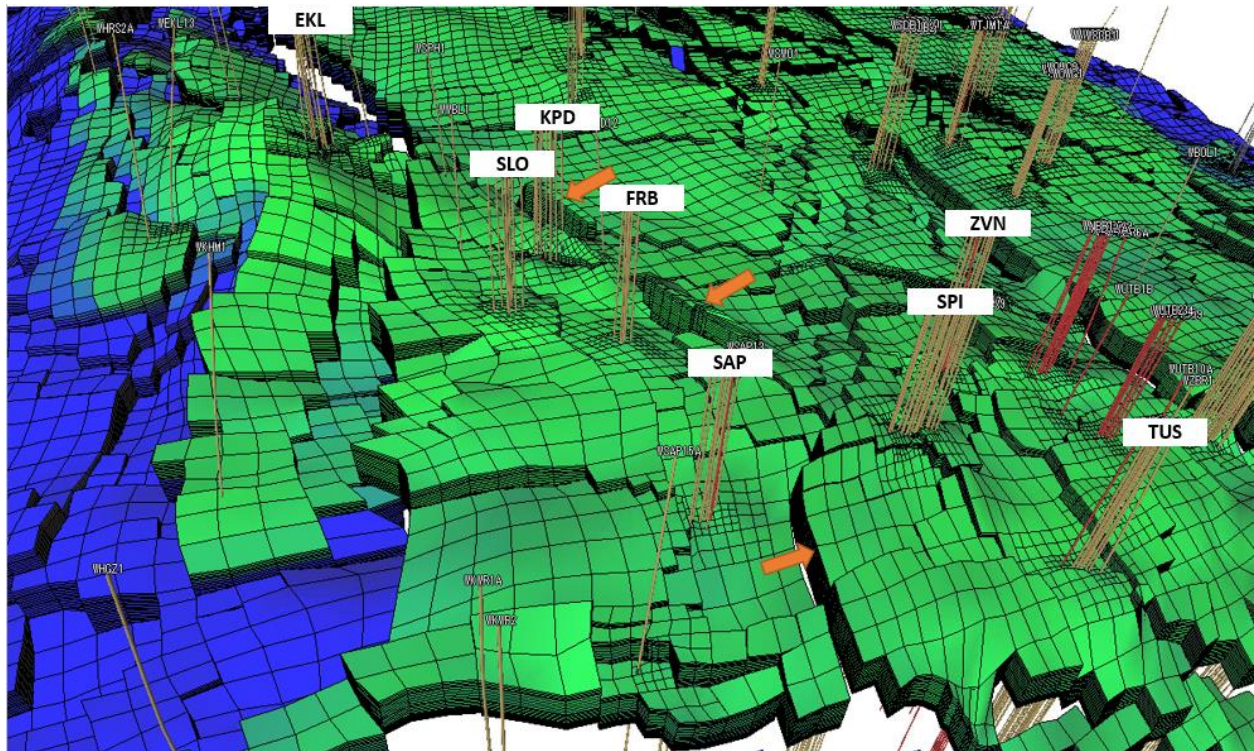


Figure 4-13: Screen capture from the Southwestern area of the V5 reservoir simulation grid, highlighting the pop-up blocks and the fault which jointly separate the area (orange arrows).

4.3.4 Kooipolder cluster fault

The CITHP data shows a pressure difference of 2 bar between the northern and southern wells of the Kooipolder cluster, see example wells KPD-6 and KPD-10A in Figure 4-14. To match this pressure difference a fault seal multiplier was introduced on the small fault running in between the cluster wells. Although the fault has a small fault throw only, as shown in Figure 4-15, a reduction in the seal factor was needed to match this observed pressure difference.

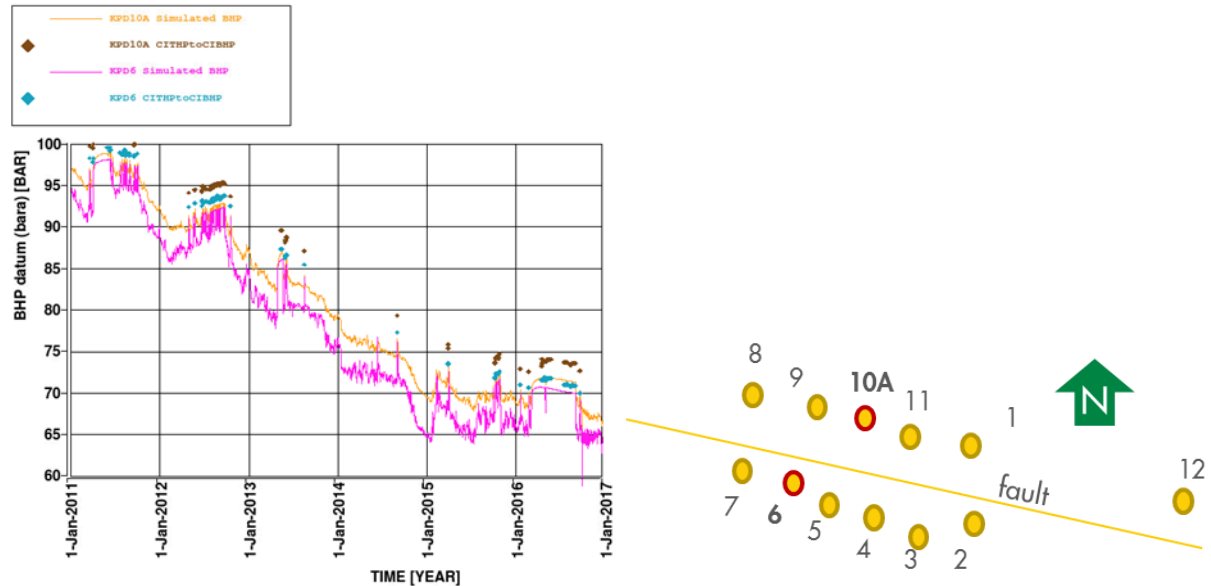


Figure 4-14 The left figure shows historic CIBHP for KPD-6 and KPD-10A versus simulated pressures from V5. The right figure sketches the subsurface location of KPD-6 and KPD-10A relative to the other cluster wells and the location of the small fault between the wells.

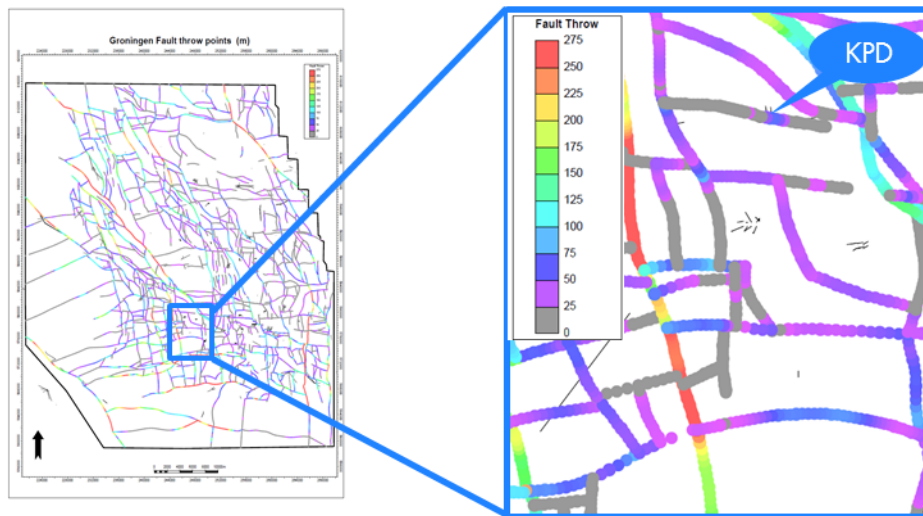


Figure 4-15 Groningen field fault throw map and zoom-in to KPD cluster area.

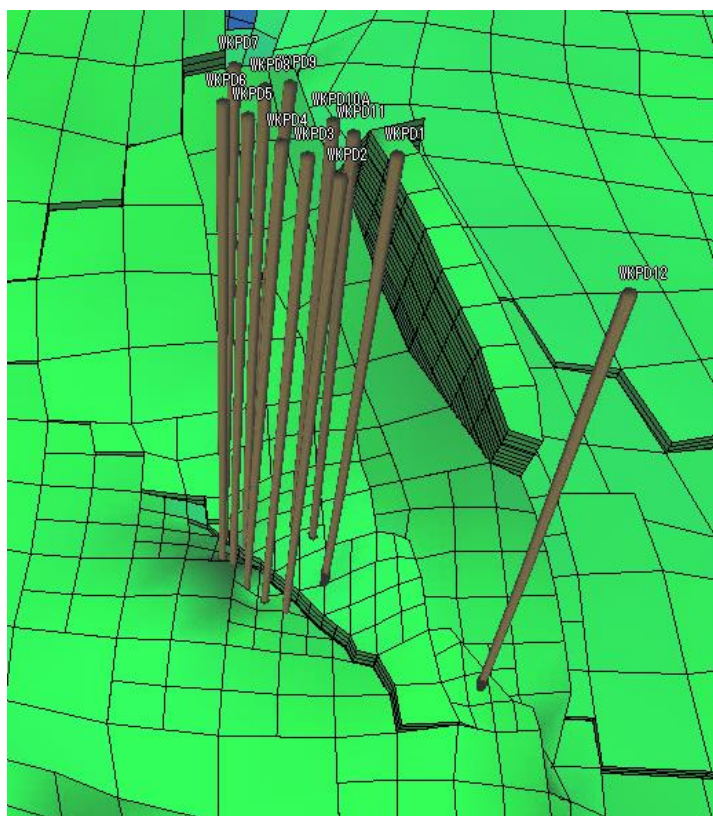


Figure 4-16: Simulation grid around the Kooipolder production cluster

4.3.5 Rodewold depletion path

The RFT data acquired in 1998 from the Rodewold-1 well (Southwestern periphery) showed depletion. In the V4 history match a depletion path was implemented via the graben separating the northwest from the southwest periphery (Figure 4-17). The V5 model utilizes an alternative depletion path in order to establish a pressure match. Depletion is implemented along the horst block via Ten Boer towards Eemskanaal.

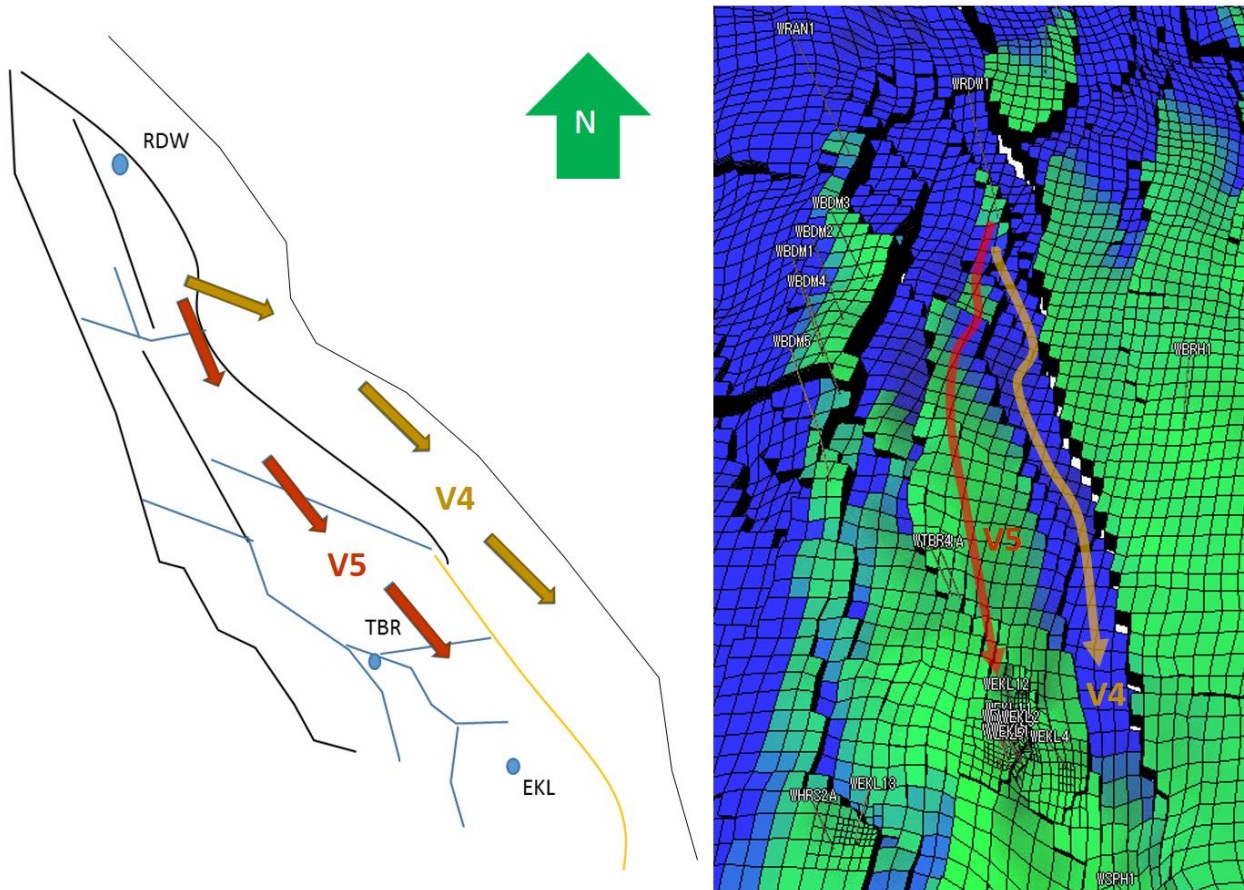


Figure 4-17: Sketch and V5 dynamic model overview showing the depletion paths of the Rodewold (RDW) well for V4 and V5 and faults in the area

4.4 In place volumes

The GIIP of the upscaled V5 static model is 2869 N.Bcm, hence identical to V4 (2868 N.Bcm). There was no update to the structural model, and only a slight increase in porosity resulting from the implementation of the second pass inversion results. Following history matching, the dynamic GIIP amounts to 2938 N.Bcm (GBV multipliers between 1.004-1.026, Figure 4-18), a slight increase compared to V4 (2934 N.Bcm).

Similar to V4, a large GBV multiplier was required (2.392) to match the Harkstede block. This is significantly higher than the GBV multipliers applied in the rest of the field. The volume in the Harkstede block is however minor compared to the rest of the field (0.6% of the dynamic GIIP) and the large multiplier can be explained by the relatively large uncertainty in the area, see Appendix 5 – Harkstede block for more detail.

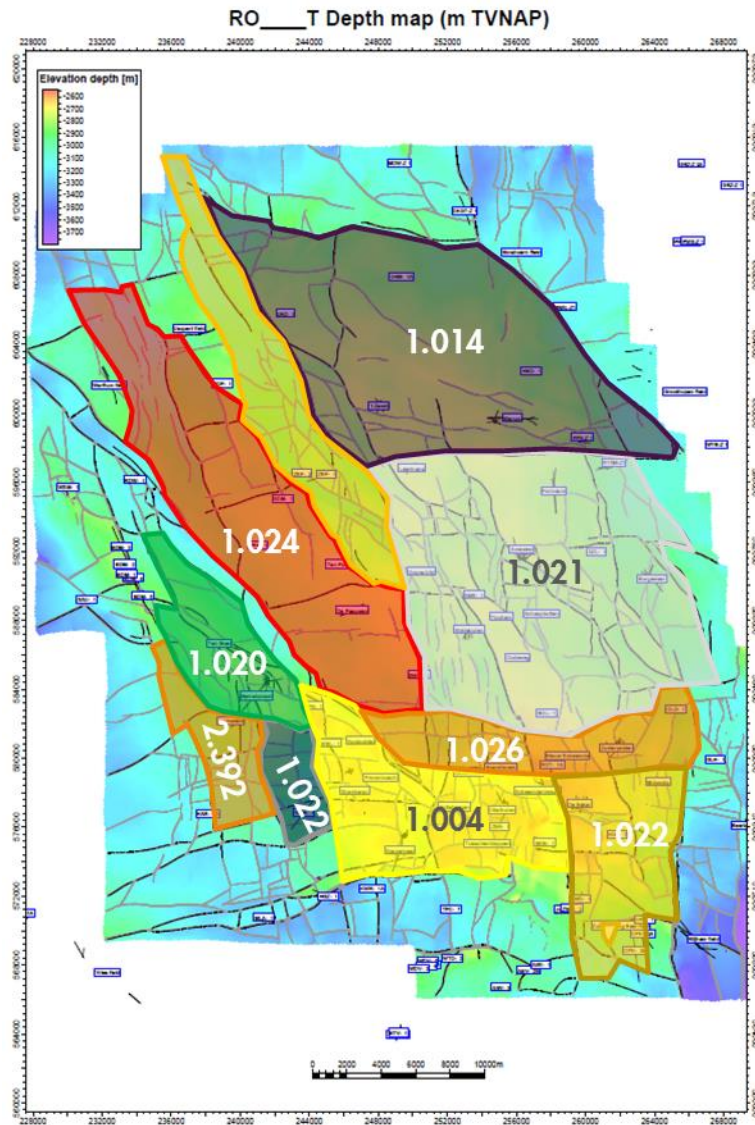


Figure 4-18 Regional gross bulk volume increases as applied in the final V5 model

4.5 Reservoir pressure match

The root mean square error to SPG data is 2.11 bar. The match to closed-in tubing-head pressure, or CITHP, for the period 2011-2017 is 1.35 bar. In their 2016 review of the V2.5 model, SGS Horizon classified a pressure mismatch less than ± 5 bar as “good”, Reference [8]. The SPG and CITHP matches on individual wells can be found in Appendix 1.

4.6 Water encroachment match

The field wide root mean square error to PNL data is 2.44 m. The PNL match on individual wells can be found in Appendix 1. The observed aquifer influx in some of the northern wells could not be satisfactorily reproduced in the model. A sensitivity in the V4 model report demonstrated potential scope for improvement by including gas in the aquifer, Reference [3]. By thus making the water leg more compressible, the bottom aquifer drive becomes more responsive.

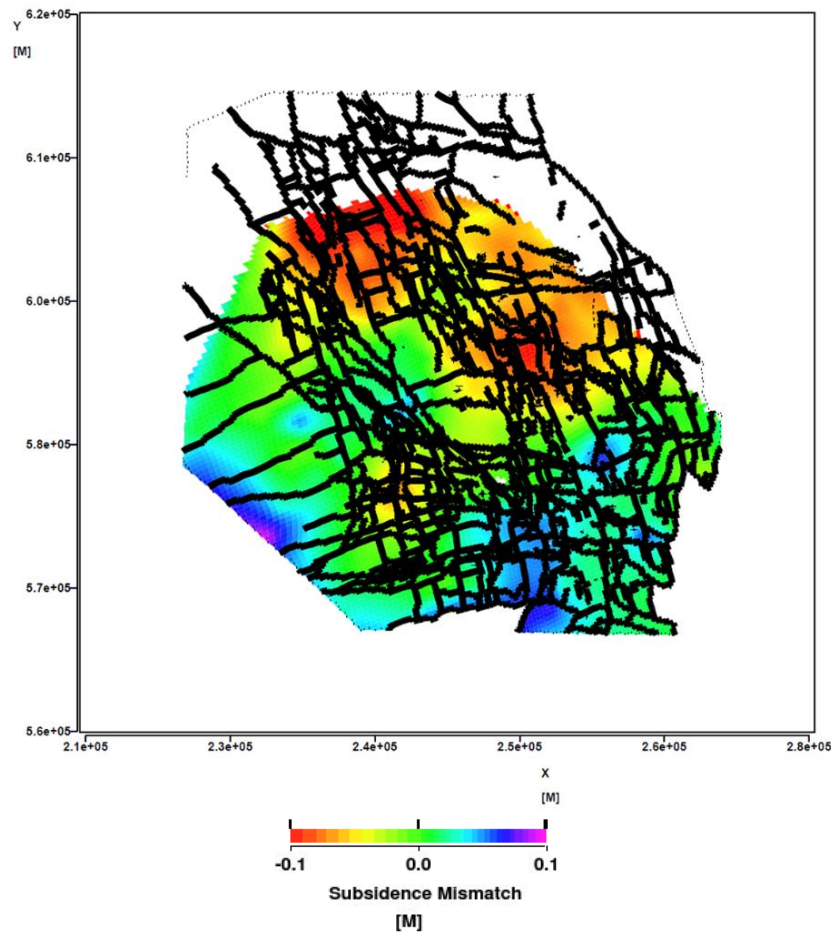
4.7 Subsidence match

V5 applies the same methodology for compressibility calculations as used in the V4 model update. In the history matching process an intermediate best match is obtained which calculates subsidence based on reservoir rock compressibility as a polynomial function of porosity. The calculated reservoir compaction due to pressure depletion is converted to surface subsidence using a proxy based on simplified overburden assumptions. The reservoir pressures from the intermediate best matched model are then fed into the high fidelity geomechanical model which is used by NAM to make subsidence predictions. Here, a subsidence inversion is done to establish the final rock compressibilities, which are loaded back into the dynamic model for the final history match. Chapter 3.3 and 5.3 in Reference [3] provide more detail on the subsidence calculations. Figure 4-19 shows a comparison of the subsidence match when using the prior versus the posterior. The V5 field-wide root mean square error for subsidence is 1.87 cm.

Subsidence mismatch = measured absolute subsidence – modelled absolute subsidence

(A) Initial compressibility estimate:

Compressibility is a polynomial function of porosity



(B) Final compressibility estimate:

Compressibility grid based on subsidence inversion

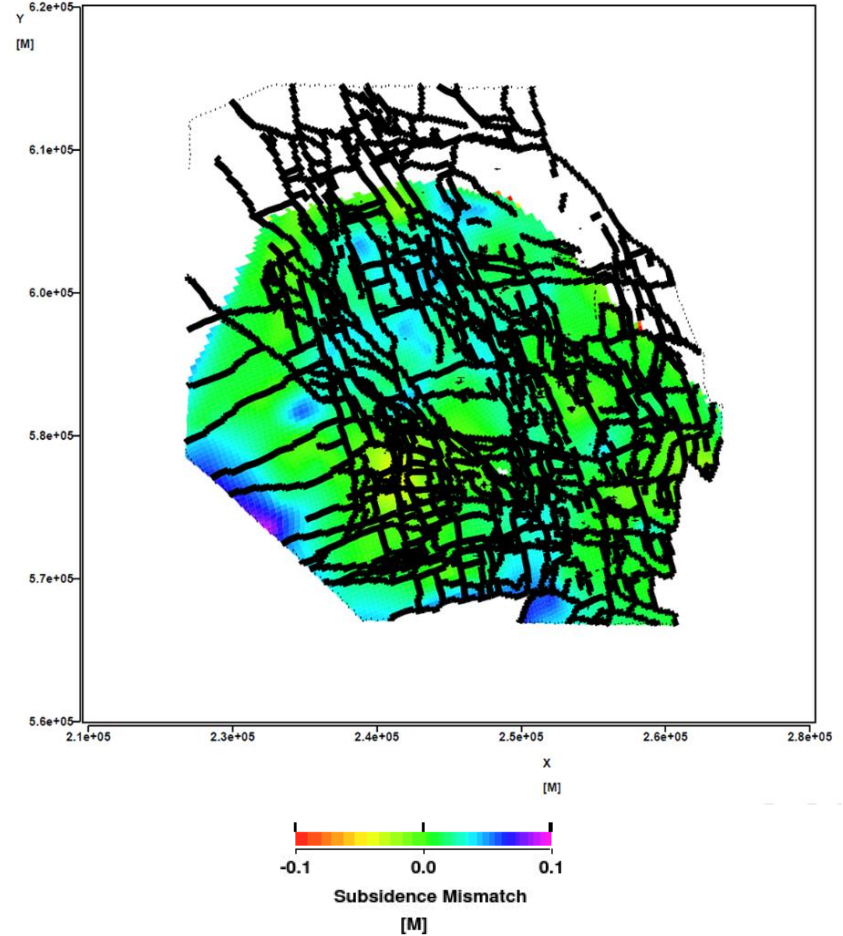


Figure 4-19 Subsidence match achieved by the V5 model for two types of compressibility, the initial polynomial function and the final inversion based grid. The figures show the subsidence mismatch as the measurement minus the model output; warm colors indicate too much subsidence, cold colors indicate too little subsidence and a good match is green.

4.8 Gravity match

V5 uses the same methodology as V4 for gravity calculations. The V5 field wide root mean square error for gravity is 5.44 μGal . Overall observations of lacking aquifer influx in the North (gas in aquifer) and lacking depletion in the South (Carboniferous) are comparable to the V4 model update [3]. The match can be found in Appendix 1.

5 Recommendations for future work

5.1 Update porosity from inversion of seismic data based on dynamic model including gas in the aquifer effects

The connectivity issues between the northern observation wells and the northern production clusters as described in V4 still exist in the V5 model after the second iteration of the seismic inversion.

For both these iterations of the seismic inversion, initial reservoir conditions were assumed [9]. However, the seismic data was acquired in 1985, by which time the reservoir had depleted by some 150 bar (reduced gas density), and water ingress up to 10-20m was observed at various places in the North of the reservoir, see the PNL match in Appendix 1. The latest seismic inversion work has found that the results are time dependent, especially due to changes in water saturation.

The seismic inversion workflow compares a modelled (synthetic) seismic signal to actual seismic data. The optimizer will adjust the synthetic seismic signal to match the actual seismic data by adjusting the reservoir thickness or porosity. Decreasing reservoir thickness or porosity will result in a lower synthetic seismic velocity, increasing reservoir thickness or porosity will result in a higher synthetic seismic velocity. If the synthetic data was constructed based on initial conditions it misses the effect of the increase in water saturation. When an increase in the water saturation is not incorporated in the seismic inversion, the inverted seismic velocity will be too low due to a too large quantity of gas. The seismic inversion workflow will then result in a decrease of porosity or reservoir thickness to create a faster synthetic signal that better matches the actual seismic data.

From model based analysis of the gravity measurements it was demonstrated that the water influx as observed from PNL logs in wells in the north of the field is a regional phenomenon, rather than local coning around individual wells [3].

In the current (and previous) model set-up it is not possible to match the water influx in the north, see the PNL match in Appendix 1. However, the sensitivity work on the effects of gas in the aquifer has shown that a large influx of water can be modeled when gas in the aquifer is incorporated [3].

The following workflow is recommended for the next model update. First match the water influx in the north of the field (e.g. by incorporating gas in the aquifer). Next, run a seismic inversion on that model realization, to create a new, unbiased porosity grid. As described earlier in this chapter, it is expected that due to the increase in water saturation in the north of the field, the seismic inversion will result in a higher porosity in that area, and thus increase connectivity.

5.2 Incorporation of Semblance and delta-thickness maps in History Matching workflow

Both semblance and delta- thickness maps provide information on the lateral spread of uncertainty in the static model. It is recommended to investigate how these maps can be used to steer areal adjustments to the static model, ideally as an integral part of the assisted history matching workflow.

5.2.1 Delta-thickness maps

Figure 5-1 shows the delta-thickness map as obtained from the seismic inversion. Because these adjustments were not implemented in the static/dynamic models, especially in places of high delta-thickness it is to be expected that the adjusted porosity alone does not fully improve the match. Where the delta-thickness map shows a positive value, the porosity should have been larger for a fixed reservoir thickness and vice-versa. Note that near the wells, porosity from well logs is preferred over porosity from seismic inversion. Therefore, large values in the delta-thickness map near wells should be ignored.

For future model updates, it is recommended to investigate the use of these delta-thickness maps in the history matching process.

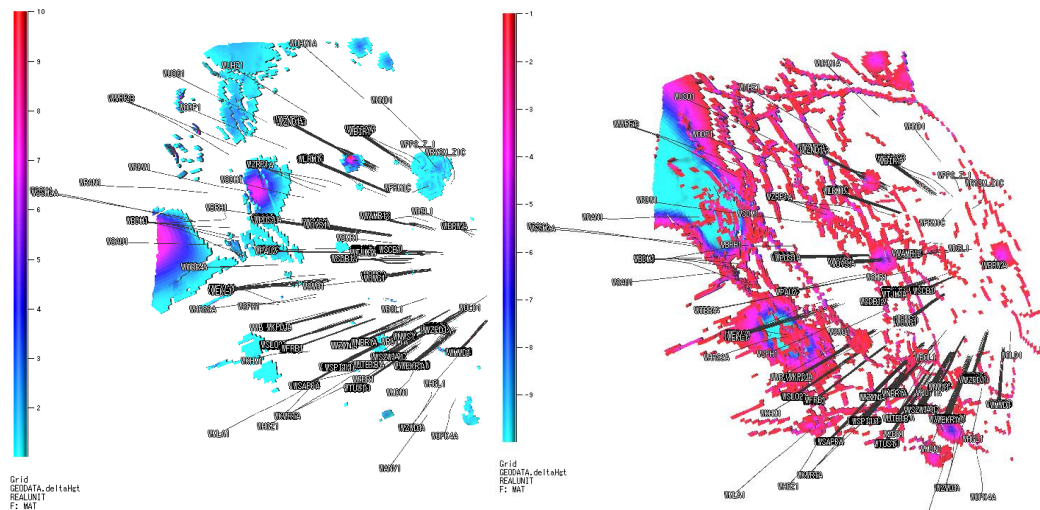


Figure 5-1 Left map shows a positive delta-thickness map for the V5 static model, indicating where porosity should be larger. The right map shows a negative delta-thickness map for the V5 static model, indicating where porosity should be smaller.

5.2.2 Semblance map

Semblance may provide an additional indication of uncertainty reservoir properties [9]. Semblance is a measure of the lateral continuity of the seismic signal and therefore the ability to track seismic horizons and determine reservoir thickness. Areas with low semblance values can be attributed to the presence of faults or to poor quality of the seismic data. This directly impacts the seismic inversion results and can be used as a measure of the associated uncertainty (i.e. a low semblance indicates a high uncertainty, and vice versa). Uncertainty in seismic data in the Groningen reservoir mainly results from the effect of floaters and salt domes in the Zechstein overlying the Rotliegend reservoir. Figure 5-2 shows a map of the semblance. In the Northeast of the field, the low semblance results from a floater with a NW-SE orientation (highlighted in yellow circle). Other low semblance areas are found in the Southeast and West of the field, reflecting the effect of the salt domes above the field.

For future model updates, it is recommended to investigate the use of semblance in the history matching process.

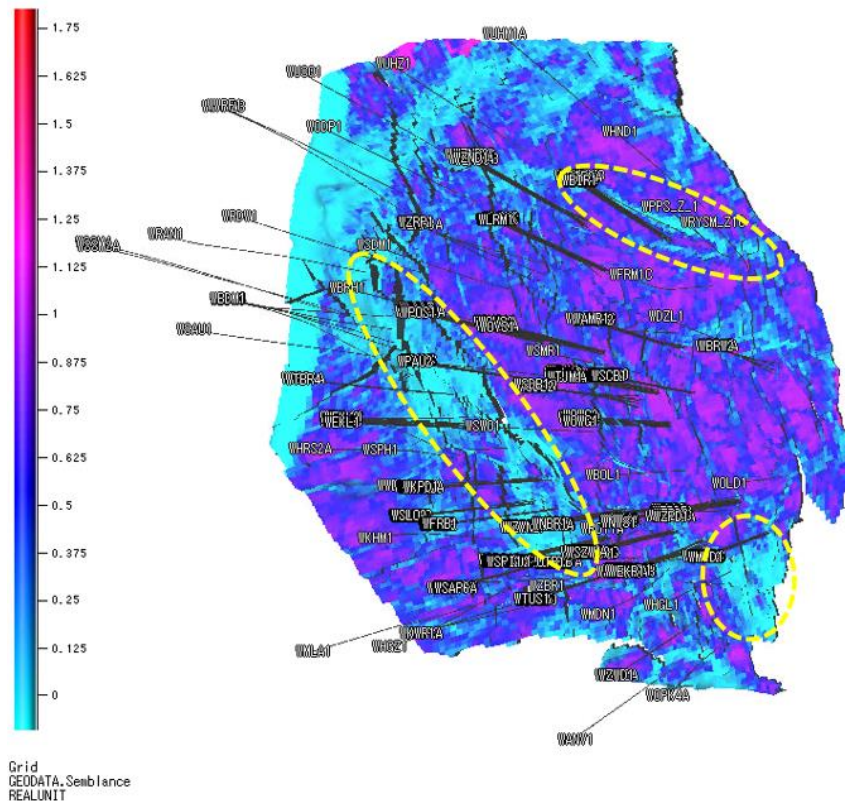


Figure 5-2 Semblance map for the V5 static model. Cold colours indicate low semblance and thus a high uncertainty.

5.3 Pre-existing recommendations

The following recommendations resulting from the V4 modelling work have not been implemented in V5, but do remain valid.

5.3.1 Gas in the aquifer

Currently, both the saturation and areal distribution of gas in the aquifer are poorly understood. Furthermore, the interpretations of the open-hole and the PNx measurements show discrepancies that need to be further reconciled before the presence of aquifer gas can be implemented in the reservoir model [10].

From a geological perspective, a description of the origin of the gas in the aquifer is required to steer the modelling of the gas distribution in the aquifer away from the wells. One hypothesis is that the gas would have migrated up from a deep source underneath the Rotliegend reservoir and some residual gas saturation got trapped on its way up to the reservoir. Available basin modelling studies [11] do report early gas charge from such a deep source rock, but also a second charge phase from a source located northwest of the Groningen field in the Lauwerszee Trough area.

5.3.2 Carboniferous

It is recommended to explore the dynamic effect of a gas bearing Carboniferous formation in the south of the field, using the dynamic reservoir simulation model. The subsidence match in the south of the field indicates that the modelled subsidence is not as much as is actually observed. This could be caused by underestimation of the matrix compressibility or by a depleting gas bearing section of the Carboniferous. Although generally very low in permeability [12], the Carboniferous in the south of the field is gas bearing, and it is measured to be lagging only 50 bars behind the main field at the HGL-1 well. The effects of a

depleting gas bearing Carboniferous need to be investigated by adding a Carboniferous interval to the static and dynamic model. Available data (e.g. reservoir properties [12] and pressure measurements in the Carboniferous [13]) can be used to populate and constrain this interval. Gas migration from the Carboniferous into the main reservoir could also explain part of the difference between static and dynamic GIP and the difference between modelled and measured gravity change.







5.3.3 Gravity data

Upon implementation of a gas-bearing Carboniferous in the dynamic reservoir model, include gravity data as a field-wide matching function in the history matching methodology [14].

6 References

- [1] U. Burkitov, H. van Oeveren and P. Valvatne, “Groningen Field Review 2015 Subsurface Dynamic Modelling Report,” NAM, Assen, 2016.
- [2] J. Van Elk and D. Doornhof, “Study and Data Acquisition Plan Induced Seismicity in Groningen for the update of the Winningsplan 2016,” NAM, Assen, March 2015.
- [3] H. Van Oeveren, P. Valvatne and L. Geurtsen, “Groningen dynamic model updates 2017,” NAM, Assen, September 2017.
- [4] Q. De Zeeuw, “Zeerijp-3 SCAL Data Review,” NAM, Assen, 2017.
- [5] J. Berre, “Special Core Analysis Review, Groningen Field,” NAM, Assen, 1990.
- [6] E. Vermolen, “Groningen SCAL data Review,” NAM, Assen, 2014.
- [7] K. van der Gijp, “Oil/Water Relative Permeability Measurements on Three Groningen Wells,” NAM, Assen, 1990.
- [8] S. Horizon, “Independent Review of Groningen Subsurface Modelling Update for Winningsplan 2016,” SGS Horizon, Voorburg, 2016.
- [9] A. Boscolo Gallo and E. Rumpfhuber, “Probabilistic seismic inversion for the Groningen field, Closing the loop,” NAM, Assen, 2017.
- [10] G. Ishmukhametova, “Investigation of gas presence in the aquifer of the Groningen field,” NAM, Assen, 2017.
- [11] S. Stevanovic, “Updated Groningen Basin Model,” SIEP, Rijswijk, 2012.
- [12] J. Seubring, “Petrophysical Evaluation of the Groningen Field Carboniferous,” NAM, Assen, 1994.
- [13] L. Vos, “Groningen Field RFT and FIT Data & Information on Limburg Connectivity,” NAM, Assen, 2003.
- [14] H. Van Oeveren, Implementation of time-lapse gravity data in the Groningen dynamic model, Assen, April 2017.
- [15] W. Miedema, “FBU Data Validation for the Groningen Field,” NAM, Assen, 2003.
- [16] “Hazard Assessment for the Eemskanaal area of the Groningen field,” NAM, Assen, 2014.
- [17] B. van Assema, “Seismic interpretation and depth conversion of Top Carboniferous in the Groningen field, northeast Netherlands,” NAM, Assen, 2017.
- [18] K. van Thienen-Visser, “Review Winningsplan Groningen,” TNO, Utrecht, 2013.

Appendix 1 – V5 best match

<p>SPG match</p> <p>RMS = 2.11 bar</p>	 GRO_2017_ED_v72_SP TG_Match.pdf
<p>RFT match</p> <p>RMS = 11.88 bar</p>	 GRO_2017_ED_v72_RF T_Match.pdf
<p>CITHP2BHP match</p> <p>RMS = 1.35 bar</p>	 GRO_2017_ED_v72_CI THP2BHP.pdf
<p>PNL match</p> <p>RMS = 2.44 meter</p>	 GRO_2017_ED_v72_P NL_Match.pdf
<p>Subsidence match</p> <p>RMS = 1.87 cm</p>	 Subsidence match V5 model for two types c
<p>Gravity Match</p> <p>RMS = 5.44 μGal</p>	 GravityMatch_Combin ed.pdf

Appendix 2 – Variable model parameter range and optimal V5 setting

	V5	Minimum	Maximum
Gross bulk volume ranges			
NorthEast_gbv_Mult	1.014	1.014	1.02
NorthWest_gbv_Mult	1.024	1.023	1.029
East_gbv_Mult	1.021	1.02	1.026
Central_gbv_Mult	1.026	1.021	1.027
SouthWest_gbv_Mult	1.004	1	1.02
SouthEast_gbv_Mult	1.022	1.02	1.026
Eemskanaal_gbv_Mult	1.02	1	1.026
Kolham_gbv_mult	1.022	1.011	1.027
Harkstede_gbv_mult	2.392	2	2.7
USQ_gbv_mult	0.99	0.975	1.025
OPK4_gbv_mult	0.96	0.955	1.025
BDM_gbv_mult	0.88	0.88	0.98
KWR_gbv_mult	1.02	0.98	1.02
FWD_gbv_mult	0.25	0.2	0.6
WRF_gbv_mult	0.945	0.94	1.01
ANV_gbv_mult	0.05	0.01	0.5
MLA_gbv_mult	0.1	0.1	1
Permeability ranges 10 ^x			
NorthEast_k_Mult	0.43	0.2	0.55
NorthWest_k_Mult	0.39	0.2	0.5
East_k_Mult	0.44	0.3	0.5
Central_k_Mult	0.69	0.4	0.7
SouthWest_k_Mult	0.44	0.3	0.5
SouthEast_k_Mult	0.4	0.3	0.5
Eemskanaal_k_Mult	0.33	0.3	0.5
Ameland_k_Mult	0	-3	0
Zeerijp_k_Mult	0.5	0.42	0.52
KWRLog_k_Mult	0.4	0.4	0.65
Feerwerd_k_Mult	-1.01	-1.2	-0.4
Warffum_k_Mult	0.54	0.4	0.6
OPK4_k_Mult	-0.95	-0.95	0.6
Fault transmissibility ranges 10 ^x			
LogFaultSeal_USQ	-1.77	-2	0
LogFaultSeal_USQgas	-5	-6	0
LogFaultSeal_ODP	-1.21	-2	0
LogFaultSeal_BRH	-1.5	-3	-1
LogFaultSeal_ZWD	-0.02	-2	0
LogFaultSeal_ANV	-6	-6	-2
LogFaultSeal_ANV_N	0	-0.2	0
LogFaultSeal_NE	-3.4	-4	-1

LogFaultSeal_NE_UHM	-0.48	-1	0
LogFaultSeal_NE_UHZ	-0.11	-2	0
LogFaultSeal_NE_ZND	-1.9	-2	0
LogFaultSeal_NE_tight	-4.55	-10	0
LogFaultSeal_ZRP	-0.18	-2	0
LogFaultSeal_BIRSouth	-0.19	-1.5	0
LogFaultSeal_BIR13	-2.84	-3	0
LogFaultSeal_RysAqf	-1.5	-2	-1
LogFaultSeal_RysAqfNorth	-1.8	-2	-1
LogFaultSeal_BRW5	-2.45	-3	-1
LogFaultSeal_AMR_LRM	-0.3	-1	0
LogFaultSeal_PopUps	-0.29	-1	0
LogFaultSeal_KPDWBL	-0.9	-1	0
LogFaultSeal_SAP_SPI	-0.2	-1	0
LogFaultSeal_TBR	-1.85	-2	-1
LogFaultSeal_TBR_w	-1.43	-6	0
LogFaultSeal_TBR_ns	-4.5	-6	0
LogFaultSeal_TBR_e	0	-6	0
LogFaultSeal_RDWN	-3.4	-6	0
LogFaultSeal_RDW	-2	-2	0
LogFaultSeal_SDBtoSZWtoEKR	-0.2	-1	0
LogFaultSeal_SPHWest	-0.55	-0.9	-0.4
LogFaultSeal_KHMTrough	-1.94	-2.2	-1.9
LogFaultSeal_Harkstede	-1.22	-2	-1
LogFaultSeal_HarkstedeNE	-0.3	-4	0
LogFaultSeal_HRS_AQF	-1.89	-2	0
LogFaultSeal_LAU	-0.24	-2	0
LogFaultSeal_HGZ	0	-0.2	0
LogFaultSeal_PosPauTjm	-0.18	-1	0
LogFaultSeal_OVSPAUSWO	-1	-1	0
LogFaultSeal_SDM	-0.89	-2	0
LogFaultSeal_OPK4	0	-2	0
LogFaultSeal_MLA	0	-0.5	0
LogFaultSeal_BDM	-8.95	-9.05	-8.05
LogFaultSeal_BDM3	-2.21	-2.76	-1.56
LogFaultSeal_BDM4	-0.34	-0.82	0
LogFaultSeal_BDM5	-0.42	-1.02	0
LogFaultSeal_RNM1	-1.93	-2.36	-1.5
LogFaultSeal_WRF1	-2	-2.5	-1.5
Negative skin uncertainty (hydraulic fractures)			
Skin_KWR1A	-3.66	-4	-3.32
Skin_SSM2A	-3	-4	-2
Skin_SSM4	-3	-4	-2
Aquifer length uncertainty			
AqfLength_AnnerveenVeendam	0	0	3000

AqfLength_Lauwersee1	6813	4000	800
AqfLength_Lauwersee2	36	0	2000
AqfLength_Lauwersee3	216	0	2000
AqfLength_Lauwersee4	942	0	6000
AqfLength_Moewensteert	11442	10000	35898
AqfLength_Rodewolt	10008	0	30000
AqfLength_Rysum	30322	0	30322
AqfLength_Usquert	12477	0	15000
AqfVsc	1.1	0.5	1.5
Relative permeability uncertainty			
Sw_unc	0	-0.05	0.05
density_gas	197	195	199
density_water	1172	1171	1173
Srg_slope	0	0	0.7
Krw_at_Srg	0.377	0.071	0.534
Krg_at_Swc	0.86	0.565	0.86
Nw	4	3.5	4.5
Ng	1.5	1.5	3
PhiMin	0.05	0.02	0.08
Min_Wat_Sat	0.45	0.26	0.6
Free water level uncertainty			
FWL_Groningen_Central	2992	2972	3012
FWL_Groningen_E	2972	2970	2972
FWL_Groningen_NE	2978	2970	2982
FWL_Groningen_NW	2984	2982	2984
FWL_Groningen_SE	3006	3003	3015
FWL_Groningen_SW	2995	2984	3006
FWL_Gron_Eemskanaal	2996	2993	2997
FWL_Gron_Ellerhuizen	2997	2970	3040
FWL_Gron_Harkstede	3016	3014	3018
FWL_Gron_Hoogezand	3030	3016	3030
FWL_Gron_Oldorp	2967	2966	2988
FWL_Gron_Zuidwending	3017	3006	3028
Compressibility and subsidence uncertainty			
Compress_rock_mult	0.58	0.55	0.61
PoissonRatio	0.25	0.24	0.26
TimeDecay	0.01	0.01	5

Appendix 3 – Model audit trail

Software

Dynamo version 2016.1 was used for all dynamic modelling work. The static Petrel model was up-scaled using flow-based upscaling in Reduce++. MoReS was used for running the numerical 3D simulation. Multirun was used as the parent for the experimental space filling design.

Location

The model is stored in the following location:

\\europe.shell.com\tcs\ams\ui.nam\field\epe_re_08\ groningen\GFR_Model_2015\20_HM\04_ExperimentalDesign_AHM\72_GRO_2017_ED_Version_72_V5_updatedSubsidence\01_SubsidenceInvertedCm

Include files (historical data, PVT, Saturation functions etc.) used by the model can be found here:

\\europe.shell.com\tcs\ams\ui.nam\field\epe_re_08\ groningen\GFR_Model_2015\Include\

Appendix 4 – Permeability comparison of reservoir model versus build-up tests

After upscaling the static model, the permeability in the dynamic model was compared to the permeability obtained from pressure transient analysis. In 2003 an overview of all available build-up test analysis results was published [15]. The distribution of permeability per cluster/location is given in Table 3.

The mean permeability from Table 3 is compared to the average permeability derived from a 3-day inflow period (Appendix 4 in Reference [3]) in the dynamic model, Figure 0-1. Locations where the PTA-derived permeability is higher are shown as a green circle, where it is lower in red. Overall, the differences stay within a factor of 3.

This comparison needs to be interpreted with some caution. Part of the differences between the model and build-up test permeabilities could be attributed to other dynamic effects, such as well bore impairment at 't-Zandt cluster, close proximity to faults in the Zuiderveen pop-up structure or high perm streaks in the central region in the field.

These observations have been used as an early check and not to constrain the posterior model permeability, for which pressure and PNL matches were used. As discussed in the V4 report [3], a permeability reduction in for instance the northern clusters relative to the permeability in the northern observation wells might be required to match the pressure behaviour in this region.

Cluster	Lognormal Distribution k[mD]				Normal Distribution k[mD]				No. Of tests
	Mean	P(15)	P(85)	Exp	Mean	P(15)	P(85)	Exp	
AMR	102	69	151	107	109	71	147	109	21
BIR	80	55	118	84	85	50	120	85	4
DZL									0
EKL	18	11	28	19	19	8	30	19	5
EKR	77	44	134	85	85	39	131	85	3
FRB	853				853				1
HND									0
HRS									0
KHM									0
KPD	65	23	182	90	91	37	145	91	13
LRM	134	115	156	135	135	114	157	135	7
MDN									0
MWD	173	138	216	178	177	141	212	177	8
NBR	377	292	486	385	383	287	479	383	2
NWS	138	121	158	139	139	122	157	139	8
OVS									0
OWG	562				562				1
PAU	349	210	579	379	384	211	556	384	5
POS	165	92	297	185	180	80	279	180	2
SAP	94	64	137	98	100	65	135	100	16
SCB	168	109	259	179	178	106	251	178	3
SDB	241				241				1
SDM	49				49				1
SLO	200				200				1
SPI	194				194				1
SZW	121	82	180	127	129	80	177	129	5
TBR									0
TJM	287	280	274	287	287	280	274	287	2
TJS	88	51	153	98	97	51	143	97	3
UTB	330	222	491	348	350	239	462	350	8
ZBR									0
ZND	79	47	133	86	88	48	127	88	7
ZPD	82				82				1
ZVN	32	11	88	44	52	0	108	53	9

Table 3: Average permeability from build-up tests per cluster/location directly copied from an overview report [15]

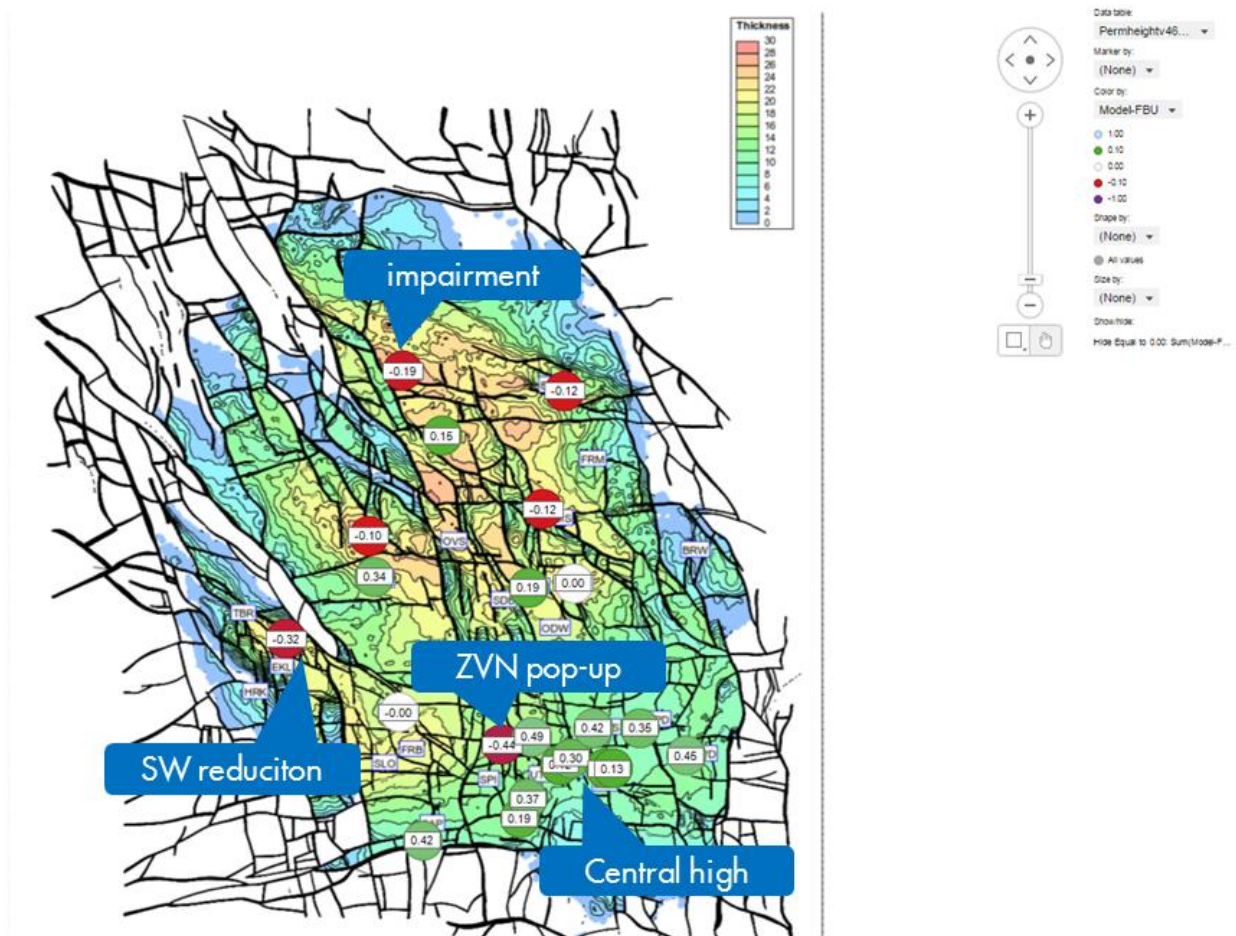


Figure 0-1 Areal overview of permeability mismatch between static model and permeability derived from build-up tests. Where the build-up test permeability is higher shows as a green circle, where it is lower in red. The permeability scaling factors are given as a power of 10 (e.g. -0.26 refers to $10^{-0.26} = 0.55$)

Appendix 5 – Harkstede block uncertainty

The GBV multiplier (2.39) in the Harkstede block is high compared to the rest of the field, but is not deemed unrealistic in light of the specific uncertainty in the area (in terms of structure and contacts), and the relatively small associated volumes (Figure 0-2). The main uncertainties are sketched in Figure 0-1 and are further explained below.

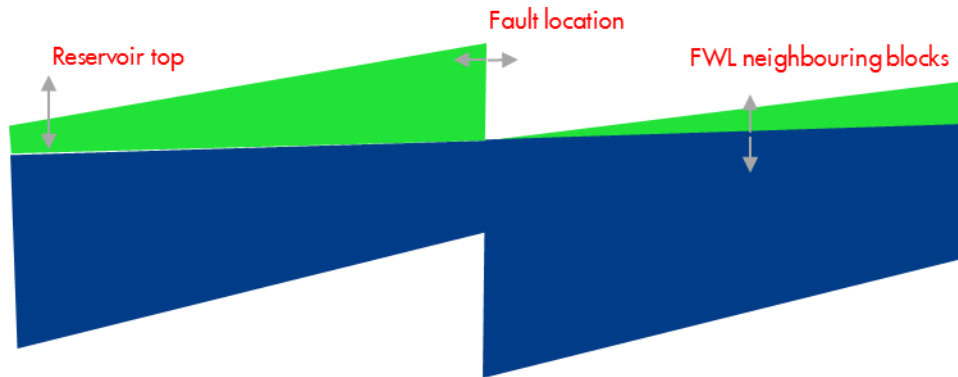


Figure 0-1 Sketch of main uncertainties impacting gas volume in the Harkstede block.

In the V5 model there are 2 main free water level regions defined around the Harkstede block, with a difference of 21 m (Figure 0-3). The area around the Harkstede block is densely faulted with significant fault offsets. A significant pressure lag is observed with the Eemskanaal area (Figure 0-2). The (partly) sealing nature of the faults in this area is poorly constrained, and leaves room for additional free water levels, given that many fault blocks in the area do not have a well penetration. A knock-on effect of the absence of well control is that the top reservoir interpretation from seismic is poorly constrained too. Figure 0-4 shows the increasing uncertainty in top-reservoir depth away from well control points. In the Harkstede block this seismic uncertainty increases to a maximum of 22 m away from the wells. In the neighbouring fault blocks without a well penetration, this is even higher. Furthermore, there is a lateral uncertainty of about 75 m in the location of mapped faults defining the lateral extent of the fault blocks. Given this combined structural uncertainty, spill points cannot help to constrain the uncertainty in free water level either.

Given this combination of factors contributing to the total uncertainty, the relatively large GBV multiplier is deemed realistic.

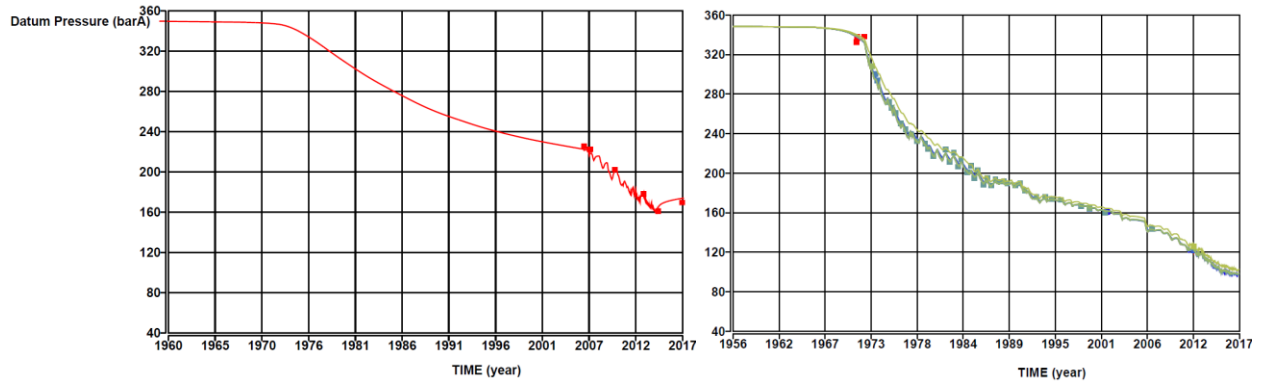


Figure 0-2 SPG pressure match for EKL-13 to the left and the other EKL cluster wells to the right.

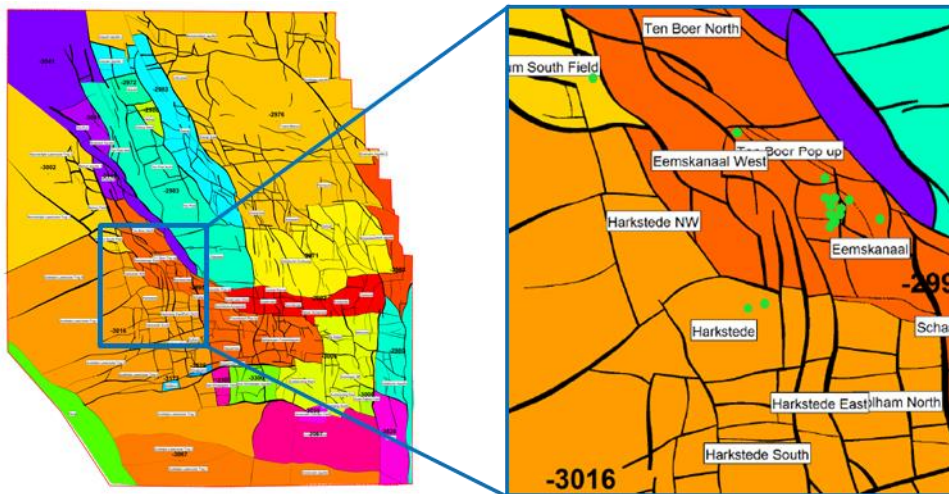


Figure 0-3 Gas water contact regions in V5 model and zoom in on Harkstede region showing a Harkstede FWL = -3016 m and Eemskanaal FWL = -2995 m. Wells are indicated by green dots.

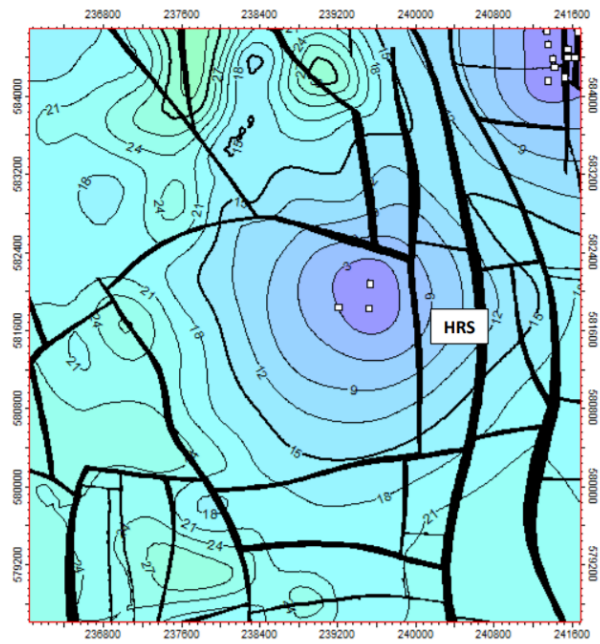


Figure 0-4 Top reservoir depth uncertainty in the Harkstede area [16]